^1H, ^{15}N, and ^{13}C NMR Signal Assignments of III^{Glc}, a Signal-Transducing Protein of *Escherichia coli*, Using Three-Dimensional Triple-Resonance Techniques†

Jeffrey G. Pelton,‡ Dennis A. Torchia,*,‡ Norman D. Meadow,§ Cing-Yuen Wong,§ and Saul Roseman§

Bone Research Branch, National Institute of Dental Research, National Institutes of Health, Bethesda, Maryland 20892, and Department of Biology and McCollum-Pratt Institute, The Johns Hopkins University, Baltimore, Maryland 21218

Received May 7, 1991; Revised Manuscript Received July 15, 1991

ABSTRACT: III^{Glc} is an 18.1-kDa signal-transducing phosphocarrier protein of the phosphoenolpyruvate:glycose phosphotransferase system (PTS) of *Escherichia coli*. Virtually complete (98%) backbone ^1H, ^{15}N, and ^{13}C nuclear magnetic resonance (NMR) signal assignments were determined by using a battery of triple-resonance three-dimensional (3D) NMR pulse sequences. In addition, nearly complete (^1H, 95%; ^{13}C, 85%) side-chain ^1H and ^{13}C signal assignments were obtained from an analysis of 3D ^{13}C HCCH-COSY and HCCH-TOCSY spectra. These experiments rely almost exclusively upon one- and two-bond *J* couplings to transfer magnetization and to correlate proton and heteronuclear NMR signals. Hence, essentially complete signal assignments of this 168-residue protein were made without any assumptions regarding secondary structure and without the aid of a crystal structure, which is not yet available. Moreover, only three samples, one uniformly ^{15}N-enriched, one uniformly $^{15}N/^{13}C$-enriched, and one containing a few types of amino acids labeled with ^{15}N and/or ^{13}C, were needed to make the assignments. The backbone assignments together with the 3D ^{15}N NOESY-HMQC and ^{13}C NOESY-HMQC data have provided extensive information about the secondary structure of this protein [Pelton, J. G., Torchia, D. A., Meadow, N. D., Wong, C.-Y., & Roseman, S. (1991) *Proc. Natl. Acad. Sci. U.S.A. 88*, 3479–3488]. The nearly complete set of backbone and side-chain atom assignments reported herein provide a basis for studies of the three-dimensional structure and dynamics of III^{Glc} as well as its interactions with a variety of membrane and cytoplasmic proteins.

The bacterial phosphoenolpyruvate:glycose phosphotransferase system (PTS) is responsible for the uptake and phosphorylation of sugars and performs an important regulatory function with respect to other processes such as diauxie. Regulation involves transduction of signals from the environment to the genome and results in the activated or repressed expression of certain genes. The *crr* gene in particular was found to be essential for this regulation, and it was shown to encode the PTS phosphocarrier protein III^{Glc}. In its phosphorylation/transport role III^{Glc} accepts a phosphate group from the cytoplasmic protein HPr at the N3 position of His-90 and thereafter donates it to the membrane-associated protein EIIB as part of a ternary glucose–EIIB–III^{Glc} complex. As a regulatory protein, III^{Glc} interacts with and modulates the activity of adenylate cyclase, glycerol kinase, and the melibose, lactose, and maltose permeases [for recent reviews, see Meadow et al. (1990), Roseman and Meadow (1990), Saier (1989), and Postma and Lengeler (1985)]. In light of its diverse functions, it is important to determine both the structure of III^{Glc} and the nature of its interactions with the range of cytoplasmic and membrane-associated proteins. As a first step, we have undertaken assignment of the NMR[1] signals of this protein using 3D double- and triple-resonance NMR spectroscopy.

Early 1D NMR investigations of PTS proteins centered around HPr (Kalbitzer et al., 1981, 1985), factor III from the lactose PTS (III^{Lac}) (Kalbitzer et al., 1982), and III^{Glc} (Dörschug et al., 1984). These studies focused on the analysis of histidyl and other aromatic resonances. With the development of 2D NMR spectroscopy, it became possible to determine the structure of HPr (Klevit et al., 1986; Klevit & Drobny, 1986; Klevit & Waygood, 1986) as well as a host of other proteins with molecular weights less than ca. 10 kDa [for reviews, see Wüthrich (1986), Kaptein et al. (1988), Clore et al. (1989), and Bax et al. (1989)].

Sequential assignment of NMR signals is the essential first step in a protein structure determination using NMR spectroscopy. With increasing molecular weight, amino acid assignments become more difficult because of severe resonance overlap. In addition, increased ^1H line widths (shorter T_2s) serve to reduce the efficiency of magnetization transfer in COSY and TOCSY experiments, making it difficult to classify ^1H spin systems according to amino acid type. The overlap problem can be significantly reduced through incorporation

† This work was supported by the AIDS Targeted Antiviral Program of the Office of the Director of the National Institutes of Health (to D.A.T.) and Grant GM 38759 from the National Institutes of Health and Grant N00014-85-k-0072 from the Office of Naval Research (to S.R.). C.-Y.W. was supported by a Predoctoral Training Grant from the National Institutes of Health and is a W. R. Grace Predoctoral Fellow. This is contribution 1465 from the McCollum-Pratt Institute.

‡ NIH.

§ Johns Hopkins University.

[1] Abbreviations: COSY, correlation spectroscopy; DANTE, delays alternating with nutation for tailored excitation; DQF-COSY, double-quantum filtered correlated spectroscopy; HCACO, proton to α-carbon to carbonyl correlation; HCA(CO)N, proton to α-carbon to nitrogen (via carbonyl) correlation; HCCH-COSY, 3D ^1H–^{13}C–^{13}C–^1H correlation via J_{cc} couplings; HCCH-TOCSY, 3D ^1H–^{13}C–^{13}C–^1H total correlation spectroscopy via isotropic mixing of ^{13}C magnetization; HMQC, heteronuclear multiple-quantum spectroscopy; HNCA, amide proton to nitrogen to α-carbon correlation; HNCO, amide proton to nitrogen to carbonyl correlation; HOHAHA, homonuclear Hartmann–Hahn spectroscopy; HSQC, heteronuclear single-quantum spectroscopy; INEPT, insensitive nuclei enhanced by polarization transfer; NMR, nuclear magnetic resonance; NOE, nuclear Overhauser effect; NOESY, nuclear Overhauser effect spectroscopy, rf, radio freqency, TOCSY, total correlation spectroscopy; 2D, two dimensional; 3D, three dimensional; $III^{Glc}N$, uniformly ^{15}N-labeled III^{Glc}_{slow}; $III^{Glc}NC$, uniformly $^{15}N/^{13}C$-labeled III^{Glc}_{slow}; $III^{Glc}SL$, III^{Glc}_{slow} containing a few amino acids labeled with ^{15}N and/or ^{13}C.

0006-2960/91/0430-10043$02.50/0

of ^{15}N- or ^{13}C-labeled amino acids combined with the application of isotope-edited 2D NMR experiments (Cross & Opella, 1985; Senn et al., 1987; Fesik & Zuiderweg, 1988; Torchia et al., 1989a; Oppenheimer & James, 1989; McIntosh et al., 1990, and references therein). Fractional deuterium labeling of nonexchangeable protons has also been used to increase both ^1H resolution and sensitivity in larger proteins (LeMaster, 1987; LeMaster & Richards, 1988; Torchia et al., 1988; Arrowsmith et al., 1990). An alternative approach has been to use J_{CC} and $J_{C'N}$ couplings to delineate spin systems and make sequential assignments by using either specific 1-$^{13}C/^{15}N$ double labels (Kainosho & Tsuji, 1982; Griffey & Redfield, 1987; Torchia et al., 1989b; Ikura et al., 1990b) or fractional $^{15}N/^{13}C$ enrichment (Stockman et al., 1988; Westler et al., 1988; Oh et al., 1988; Stockman et al., 1989; Niemczura et al., 1989). Recently, the development of 3D homonuclear (Vuister et al., 1988; Oschkinat et al., 1988, 1989), 3D heteronuclear (Fesik & Zuiderweg, 1988; Marion et al., 1988a,b; Zuiderweg & Fesik, 1989; Ikura et al., 1990c), and 4D heteronuclear NMR spectroscopy (Kay et al., 1990c; Clore & Gronenborn, 1991; Clore et al., 1991) have extended the size of proteins that can be analyzed by spreading connectivity information into additional frequency dimensions.

III^{Glc} presented a particular assignment challenge because of its size (18.1 kDa) and the fact that it contains a large number of similar residues. For example, 50 of the 168 amino acids are either Val (19), Ile (19), or Leu (12). In addition, III^{Glc} contains 17 lysine and 3 arginine residues whose side-chain protons generally show poor chemical shift dispersion. For these reasons, we have adopted an assignment strategy recently demonstrated by Bax and co-workers and applied to calmodulin (Ikura et al., 1990c, 1991). With these experiments, we were able to combine the spectral dispersion provided by triple-resonance 3D NMR (Kay et al., 1990a) with the ease of uniform $^{15}N/^{13}C$ labeling to sequentially assign the ^1H, ^{15}N, and ^{13}C backbone signals. At the same time, we identified the amino acid spin systems using HCCH-COSY (Kay et al., 1990b; Bax et al., 1990a; Clore et al., 1990) and HCCH-TOCSY (Bax et al., 1990b; Clore et al., 1990) spectra using the same uniformly enriched samples. Together, these data provided for virtually complete ^1H, ^{15}N, and ^{13}C resonance assignments for III^{Glc}. Moreover, since these 3D experiments rely solely on J couplings, the assignments were made without reference to NOE information or assumptions about structure. Previously we reported on the secondary structure of III^{Glc} determined through analysis of ^{15}N and ^{13}C 3D NOESY-HMQC spectra (Pelton et al., 1991). Herein, we report the ^1H, ^{15}N, and ^{13}C backbone and side-chain resonance assignments.

Materials and Methods

Growth of Bacteria and Purification of III^{Glc}. The coding sequence of the *crr* gene was cloned into the *Nde*I–*Eco*RI sites of pVEX-11 (a gift from Dr. V. Chaudhary, Laboratory of Molecular Biology, National Institutes of Health) under the control of the T7 promoter. *E. coli* strain BL21 (DE3) (Studier & Moffatt, 1986) was transformed with plasmid pVEX-*crr* and grown in the minimal medium of Neidhardt et al. (1974), with 0.2% glucose as the carbon source and supplemented with 2 mg/mL thiamine and 50 mg/mL ampicillin. Uniformly enriched ^{15}N and $^{15}N/^{13}C$ samples were obtained by growing bacteria on either $^{15}NH_4Cl$ as the sole nitrogen source or $^{15}NH_4Cl$/glucose-$^{13}C_6$ as the sole nitrogen and carbon sources, respectively. A third sample was prepared by growing bacteria on 1.5 L of medium containing 40.6 mg of [^{15}N, 1-^{13}C]D,L-Leu, 26.9 mg of [5,5-$^{13}C_2$]D,L-Leu, 20.3 mg of [^{15}N]L-Phe, 59.5 mg of [3-^{13}C]D,L-Phe, 100.3 mg of [^{15}N]L-Lys, 100.9 mg of [1,2-^{13}C]Gly, 40.1 mg of [1-^{13}C]L-Ile, 59.1 mg of L-Ile(unlabeled), 20.9 mg of [^{15}N,2-^{13}C]L-Pro, 4.5 mg of [^{15}N]D,L-His, 11.6 mg of [1,3-$^{15}N_2$]D,L-His, and all other amino acids (100 mg) except serine, which was withheld from the medium. The ^{15}N, $^{15}N/^{13}C$, and specifically labeled samples will hereafter be denoted $III^{Glc}N$, $III^{Glc}NC$, and $III^{Glc}SL$, respectively. Examination of ^{13}C HMQC spectra of $III^{Glc}SL$ with and without $^{13}C'$ decoupling revealed that serine was partially labeled at all three positions as a result of cross labeling from [1,2-^{13}C]Gly. No other signals resulting from cross labeling were observed. When cultures reached an absorbance of 2–2.5 OD (500 nm), synthesis of III^{Glc} was induced by adding isopropyl β-D-thiogalactoside (1 mM). The cells were harvested after an additional 2 h of growth.

The cells were harvested by centrifugation and washed once in the medium of Neidhardt et al. (1974) without the addition of any supplements or nitrogen. The cell pellet was then resuspended to 0.2 g/mL (wet weight) of the same medium to which *p*-aminobenzamidine, 2-deoxyglucose, and KF (each 10 mM) were added. This suspension was incubated for 15 min at 36.5° to discharge phosphoryl groups from the III^{Glc} and then frozen until use, usually overnight. All of the following steps were performed at 0–4 °C. Streptomycin sulfate (10% in H_2O) was added to the thawed homogenate (to a concentration of 1.3%), which was then incubated for 15 min and centrifuged for 1 h at 200000*g*. The supernatant was diluted to 500 mL with 50 mM BisTris [2-[bis(2-hydroxyethyl)amino]-2-(hydroxymethyl)-1,3-propanediol] (pH 6.5 at 0 °C), and 10 mM *p*-aminobenzamidine (titrated with Tris base to pH 6.5) (buffer A) and loaded onto a 730-mL (6 × 26 cm) column of DEAE Sepharose 6B-CL (Pharmacia) at a flow rate of 5 mL/min. The column was washed with 500 mL of buffer A, then with 1500 mL of buffer A containing 50 mM KCl, followed by a 4-L gradient of 50–300 mM KCl in buffer A. The III^{Glc} eluted after about 2600 mL of the gradient had entered the column.

The fractions containing III^{Glc} (detected by fused rocket immunoelectrophoresis (Meadow & Roseman, 1982) were concentrated to 7–8 mL with a 10000 MW cut-off ultrafiltration membrane (Pellicon, Millipore), made to 6.3% (w/v) glycerol, and loaded onto a 500-mL (2.6 × 95 cm) column of Sephacryl S-200 (Pharmacia) equilibrated with 50 mM Tris-HCl (pH 7.9 at 4 °C), 1 mM EDTA, 3.8% (w/v) glycerol, and 0.05% NaN_3 and developed at a flow rate of 0.85 mL/min. The III^{Glc} containing fractions were analyzed by SDS–polyacrylamide gel electrophoresis and pooled on the basis of purity. Approximately 25, 25, and 40 mg of III^{Glc} were obtained from the ^{15}N, $^{15}N/^{13}C$, and specifically labeled preparations, respectively, per liter of medium. The purity of each sample was greater than 97% based on SDS–PAGE followed by quantitative densitometric scanning of the Coomassie-stained gel. For spectra recorded in D_2O, amide protons were exchanged for dueterions by heating the sample overnight (42 °C) and subsequently reheating it (48 °C) for 18 h. Each sample contained 1.6 mM III^{Glc} in 0.15 M KCl (pH 6.4 uncorrected for isotope effects) and either 90% H_2O/10% D_2O or 99.996% D_2O (Cambridge Isotope labs, Woburn, MA).

NMR Spectroscopy. All NMR experiments were recorded at 36.5 °C on an AM-500 spectrometer modified to reduce overhead time at the end of each (t_1,t_2) increment (Kay et al., 1990a). For spectra recorded in H_2O, a DANTE pulse sequence with an effective field strength of ca. 25 Hz was used to suppress the solvent signal (Kay et al., 1989). No presa-

turation was used for experiments acquired in D_2O.

2D NMR Spectroscopy. Homonuclear DQF-COSY (Rance et al., 1983) and TOCSY/HOHAHA (Braunschweiler & Ernst, 1983; Bax & Davis, 1985) spectra of III^{Glc}SL were recorded in D_2O for the purpose of assigning the eight Phe aromatic spin systems. In both experiments, 32 scans were signal averaged for each of 1024 t_1 points. The carrier was set to 4.66 ppm, and acquisition times in both dimensions were 85 ms. For the TOCSY/HOHAHA experiment, a WALTZ-16 pulse sequence (Shaka et al., 1983) was applied for 33 ms. The data were processed with a Lorentzian-to-Gaussian filter in t_1 and t_2 prior to Fourier transformation. The final digital resolution was 5.9 Hz per point in each dimension.

2D ^{15}N HSQC spectra of III^{Glc}N and III^{Glc}SL were acquired in H_2O with the Overbodenhausen pulse sequence (Bax et al., 1990c). ^1H decoupling was achieved with a 180° pulse in the middle of the t_1 time period, and ^{15}N decoupling was achieved with WALTZ-16 modulation of a 1 kHz rf field in t_2. A total of 16 transients were signal averaged for each of 800 t_1 values. Acquisition times were 200 ms (t_1) and 128 ms (t_2), respectively. The data were processed with a Lorentzian-to-Gaussian filter in both dimensions. The final digital resolution was 2 Hz per point in F_1 and 4 Hz per point in F_2.

2D ^{13}C HMQC (Bax et al., 1990c) and ^{13}C HMQC-NOESY (Gronenborn et al., 1989; Shon & Opella, 1989) spectra of III^{Glc}NC and III^{Glc}SL were recorded in D_2O. In both experiments WALTZ-16 modulation of an 800-Hz field centered at 177 ppm was used for $^{13}C'$ decoupling in t_1, and GARP (Shaka et al., 1985) modulation of a 4-kHz rf field centered at 43.0 ppm was used for $^{13}C\alpha$ decoupling in t_2. A total of 48 transients were signal averaged for each of 800 t_1 points with acquisition times of 57.6 ms (t_1) and 128 ms (t_2 HMQC) or 102.4 ms (t_2 HMQC-NOESY), respectively. The ^{13}C carrier was set to 43.0 ppm and the ^1H carrier was set to 2.80 ppm (HMQC) or 4.67 ppm (HMQC-NOESY). A 100 ms mixing time was used in the HMQC-NOESY experiment. The data were processed similarly to HSQC spectra. The final digital resolution was 13.6 Hz per point in F_1 and 4.0 Hz (HMQC) or 4.9 Hz (HMQC-NOESY) per point in F_2.

3D NMR Spectroscopy. In all of the 3D experiments described below, quadrature data were collected in t_1 and t_2 according to the TPPI-States method (Marion et al., 1989c). 3D data sets were transferred to a SUN4-110 workstation (SUN Microsystems Inc., Milpitas, CA) and processed with a combination of in-house and commercial software (Marion et al., 1989; Kay et al., 1990; NMRi, Syracuse, NY). A sine-bell filter was applied in t_1 and t_2, and a sine-bell squared filter was applied in the third (t_3) dimension of each experiment with phase shifts ranging from 45° to 60°. The data matrices were zero-filled twice in t_1 and once each in t_2 and t_3 before Fourier transformation.

3D HOHAHA-HMQC experiments were recorded on III^{Glc}N at pH 6.4 by using the sequence of Marion et al. (1989b) and at pH 7.0 by using a modified pulse sequence as follows: with phase cycling ϕ_1, 4(x,$-x$); ϕ_2, 4(x) 4(y); ϕ_3,

$$^1H\ \text{WM–DANTE–}90°_{\phi 1}\text{–}t_1\text{–TR–}t_m\text{–TR–}90°_x\text{–}t\text{–}90_{\phi 2}\text{—}180°_x\text{—acq}$$
$$^{15}N\qquad\qquad\qquad\qquad\qquad\qquad\qquad\qquad\Delta\text{–}90°\psi\text{–}t_2\text{–}90_{\phi 3}\text{–}\Delta$$

2(x,x,$-x$,$-x$); acq, (x,$-x$,$-x$,x,$-y$,y,y,$-y$) (A. Bax, personal communication). The warmup period (WM) consisted of a 36-ms spin-locking rf field that was applied at the beginning of each t_1 increment. Trim pulses (TR) were applied for 2 ms. Mixing was achieved with a DIPSI-2 sequence (Shaka et al., 1988) and was applied for 36 ms. The delay t (9 ms) was used to remove rotating-frame NOE effects, and the delay Δ (4.5 ms) was set to slightly less than $1/2J_{NH}$. For each t_1 increment, ϕ_1 and the receiver were incremented by 180°, and, for each t_2 increment, ψ and the receiver were incremented by 180°. Data obtained for $\phi_1(x,y)$ and $\psi(x,y)$ were stored separately as complex data. The ^1H carrier was set to 4.67 ppm (H_2O), and the ^{15}N carrier was set to 118.5 ppm. A WALTZ-16 pulse sequence was used to decouple ^{15}N during t_3. The spectrum was derived from a 128 (complex) × 32 (complex) × 1024 (real) data matrix with acquisition times of 25.6 ms (^1H t_1), 27.5 ms (^{15}N t_2), and 64 ms (^1H t_3), respectively. A total of 64 scans were recorded per (t_1,t_2) point.

HNCA and HNCO spectra (Ikura et al., 1990c; Kay et al., 1990a) were recorded in H_2O. In both experiments carrier frequencies were set as follows: ^1H 4.67 ppm; ^{15}N 118.5 ppm; $^{13}C\alpha$ 56 ppm; $^{13}C'$ 176.5 ppm. Recycle and ^{15}N–^1H INEPT delays were set to 1.0 s and 2.25 ms, respectively. The data matrix resulted from 32 (complex) × 64 (complex) × 1K (real) points in t_1, t_2, and t_3, respectively. For the HNCA experiment, acquisition times were 27.5 ms (^{15}N t_1), 14.8 ms ($^{13}C\alpha$ t_2), and 63.5 ms (NH t_3). The fixed delay during which ^{15}N and $^{13}C\alpha$ signals become antiphase was set to 22 ms. A 500-Hz $^{13}C'$ rf field modulated with WALTZ-16 was used to decouple $^{13}C'$ spins during t_2. A total of 128 scans were recorded for each (t_1,t_2) value with a phase cycle of 32 scans. For the HNCO experiment, acquisition times were 27.5 ms (^{15}N t_1), 38 ms ($^{13}C'$ t_2) and 63.5 ms (^1H t_3). The fixed delay during which ^{15}N and $^{13}C'$ signals become antiphase was set to 18 ms. A total of 64 scans were recorded per (t_1,t_2) value with a phase cycle of 16 scans.

HCACO and HCA(CO)N spectra (Ikura et al., 1990c; Kay et al., 1990a) were recorded in D_2O. In both experiments, the carrier frequencies were set as follows: ^1H 3.85 ppm; $^{13}C\alpha$ 56 ppm; ^{15}N 118.5 ppm. Pulses applied to the $^{13}C'$ spins were generated by using an off-resonance DANTE pulse sequence as described (Kay et al., 1990a). Recycle, $^{13}C\alpha$–^1H INEPT, and $^{13}C\alpha$–$^{13}C'$ refocusing delays were set to 0.8 s, 1.5 ms, and 3 ms, respectively. Both data matrices resulted from 32 (complex) × 64 (complex) × 512 (real) points in t_1, t_2, and t_3. For the HCACO experiment, acquisition times were 10.6 ms ($^{13}C\alpha$ t_1) 38.4 ms ($^{13}C'$ t_2), and 51.2 ms (^1H t_3). A total of 64 scans per (t_1,t_2) point were signal averaged by using a 16-step phase cycle. During t_2, ^{15}N decoupling was achieved with WALTZ-16 modulation of a 1 kHz rf-field. For the HCA(CO)N experiment, acquisition times were 10.6 ms ($^{13}C\alpha$ t_1) 55 ms (^{15}N t_2), and 51.2 ms (Hα t_3) with the fixed delay during which $^{13}C'$ and ^{15}N become antiphase set to 20 ms. A total of 128 scans were recorded per (t_1,t_2) value with a 32-step phase cycle.

HCCH-COSY (Kay et al., 1990b; Bax et al., 1990a) and HCCH-TOCSY (Bax et al., 1990b; Clore et al., 1990) spectra of III^{Glc}NC were recorded in D_2O. In both experiments, the ^1H and ^{13}C carrier frequencies were set to 2.8 and 43 ppm, respectively. A recycle delay of 0.75 s was used. All fixed delays were the same as those described (Bax et al., 1990a,b). Both data matrices resulted from 64 (complex) × 32 (complex) × 512 (real) data matrices with acquisition times of 21.4 ms (^1H t_1), 10.6 ms (^{13}C t_2), and 51.2 ms (^1H t_3). The ^{13}C spectral width of 2994 Hz resulted in extensive folding of signals; however, this caused few signal overlap problems because ^1H and ^{13}C chemical shifts are well correlated. For the HCC-H-COSY spectrum, 64 scans per (t_1,t_2) increment were recorded with a 16-step phase cycle. For the HCCH-TOCSY spectrum, 128 scans per (t_1,t_2) increment were recorded with a 32-step phase cycle and a mixing time of 24 ms.

Both in-house and commercial software (NMRi, Syracuse, NY) were used to peak pick the various 2D and 3D spectra. Chemical shifts are referenced to H_2O (4.67 ppm, 36.5 °C), external liquid ammonia (^{15}N), and sodium 3-[2,2,3,3-$^2H_4$]-trimethylsilylpropionate (^{13}C) (Live et al., 1984). Uncertainties in chemical shifts are 0.02 and 0.1 ppm for ^1H and heteronuclei, respectively.

RESULTS

Identification of Intraresidue Backbone ^1H, ^{15}N, and ^{13}C Signals. In a ^{15}N HSQC spectrum of $III^{Glc}N$ (supplementary material), we identified 166 out of an expected 171 signals, taking into account that III^{Glc} contains seven Pro, four Asn, and one Gln (Table I). Four of the five missing resonances correspond to those of Gly-1, Leu-2, Asn-57, and Ser-83, which remain unassigned. The last signal is accounted for by the fact that G65 and G18 have identical ^{15}N and ^1H chemical shifts. Moreover, the signals in this spectrum showed excellent chemical shift dispersion in both the ^{15}N and ^1H dimensions, which greatly facilitated the assignment process. In only three cases were the ^{15}N and ^1H signals of two residues separated by 0.2 ppm or less and 0.02 ppm or less, respectively.

Comparison of ^{15}N HSQC spectra acquired several weeks apart revealed several new resonances that grew in intensity over time. Previously it was noted (Studier & Moffatt, 1986) that two forms of III^{Glc}, designated III^{Glc}_{fast} and III^{Glc}_{slow}, were isolated during purification, and it was shown that III^{Glc}_{fast} results from cleavage of the N-terminal heptapeptide of III^{Glc}_{slow} by a membrane-associated endopeptidase (Meadow et al., 1986). Results from polyacrylamide gel electrophoresis showed that the sample had converted from the slow to the fast form over the period of data collection (several weeks), presumably due to a slight contamination of the III^{Glc} by the endopeptidase, and we therefore attributed the new resonances to cleavage products. Since *p*-aminobenzamidine inhibits the endopeptidase, new samples were prepared and purified as stated above except that they were also applied to a *p*-aminobenzamidine–agarose column (Sigma), which significantly slowed the rate of proteolysis of the III^{Glc}_{slow} in the eluate. Comparison of ^{15}N and ^1H chemical shifts for the slow and fast forms of III^{Glc} revealed no changes except for residues near the cleavage site. This is because the first 18 residues of III^{Glc}_{slow} are disordered and do not interact with the remainder of the protein (Pelton et al., 1991). Thus, although proteolysis of the disordered N-terminus occurred during data acquisition, we were able to assign the resonances of the intact form (III^{Glc}_{slow}) of the protein with the exception of residues Asp-4–Ser-8.

The ^{15}N–^1H signals derived from the HSQC spectrum were used as a starting point for intraresidue backbone ^{15}N, ^{13}C, and ^1H assignments (Table I) using the 3D ^{15}N HOHAHA-HMQC (Marion et al., 1989b) and the 3D triple-resonance HNCA and HCACO (Ikura et al., 1990c; Kay et al., 1990a) experiments. The 3D ^{15}N HOHAHA-HMQC experiment is derived from the 2D HOHAHA/TOCSY and HMQC experiments. Cross peaks in this spectrum correlate the ^{15}N–^1H signal of each residue with intraresidue side-chain protons (Figure 1). In all, we matched approximately 75% of the ^{15}N–^1H correlations identified in the HSQC spectrum with the corresponding Hα signals. The remaining Hα resonances either were saturated along with the solvent by the off-resonance DANTE pulse sequence or were not observed because of small NH–Hα *J* couplings. In addition, we identified at least one Hβ signal in 70% of the cases, which proved useful in completing the intraresidue assignments (see below). However, because of the relatively short T_2s for protons within a protein of this size, most correlations to Hγ, Hδ, and Hϵ protons were not observed.

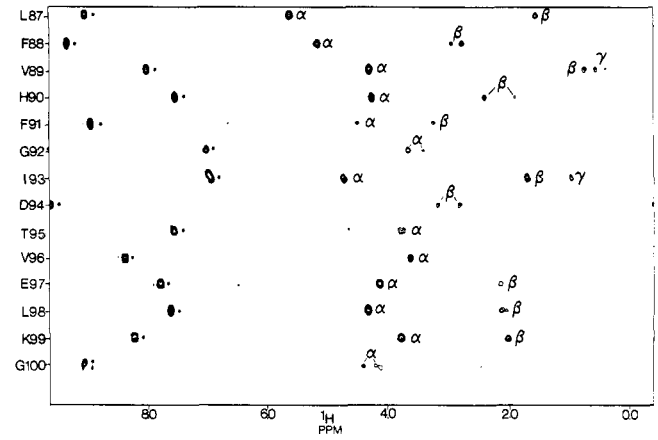

FIGURE 1: Composite spectrum consisting of strips taken from ^{15}N planes of a 3D ^{15}N HOHAHA-HMQC spectrum of $III^{Glc}N$ acquired with a mixing time of 36 ms (36.5 °C, pH 6.4). Diagonal (asterisks) and intraresidue side-chain ^1H signals (greek letters) are shown for residues L87–G100.

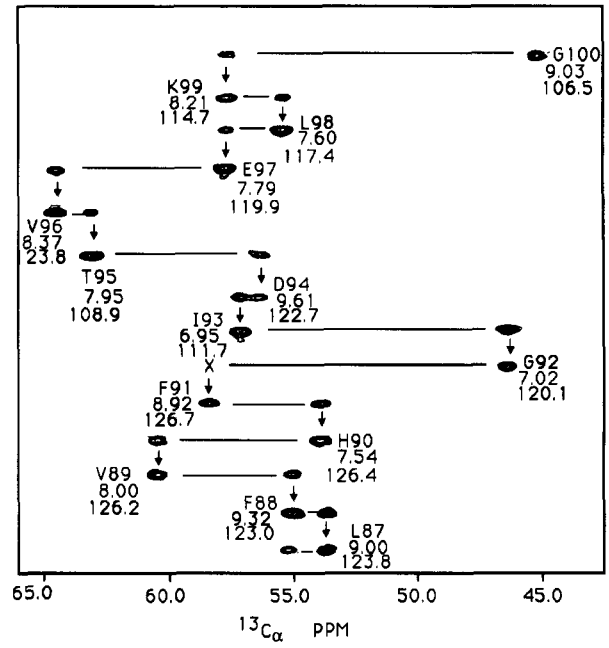

FIGURE 2: Composite spectrum consisting of strips taken from ^{15}N planes of a 3D HNCA spectrum of $III^{Glc}NC$ for residues L87–G100. Intraresidue ^1H–^{15}N–$^{13}C\alpha$ correlations are denoted by residue label and both ^{15}N and NH chemical shifts. Arrows indicate interresidue $^{13}C\alpha_{i,i-1}$ correlations. The letter X is used to indicate those $C\alpha_{i-1}$ signals that were not observed.

The HNCA experiment links each ^{15}N–^1H correlation with the intraresidue $^{13}C\alpha$ signal and in many cases with the $^{13}C\alpha$ signal of the preceding residue (Ikura et al., 1990c; Kay et al., 1990a) (Figure 2). In general, the intraresidue $^{13}C\alpha$–^{15}N coupling constant ($\approx$ 11 Hz) is larger than the two-bond $^{13}C\alpha$–^{15}N coupling constant ($\approx$ 7 Hz), and, therefore, intraresidue correlations can usually be distinguished from those to the preceding residue by a comparison of peak intensities. For example, in Figure 2, the ^{15}N–^1H pair of His-90 is correlated by a strong cross peak with its own $^{13}C\alpha$ signal at 53.9 ppm and by a weaker cross peak to the $^{13}C\alpha$ signal of the preceding residue (V89) at 60.6 ppm. In a few cases (10%), both cross peaks were of equal intensity, making it difficult to assign the intraresidue signals. One way to resolve these ambiguities is to acquire the spectrum with a shorter ^{15}N–$^{13}C\alpha$

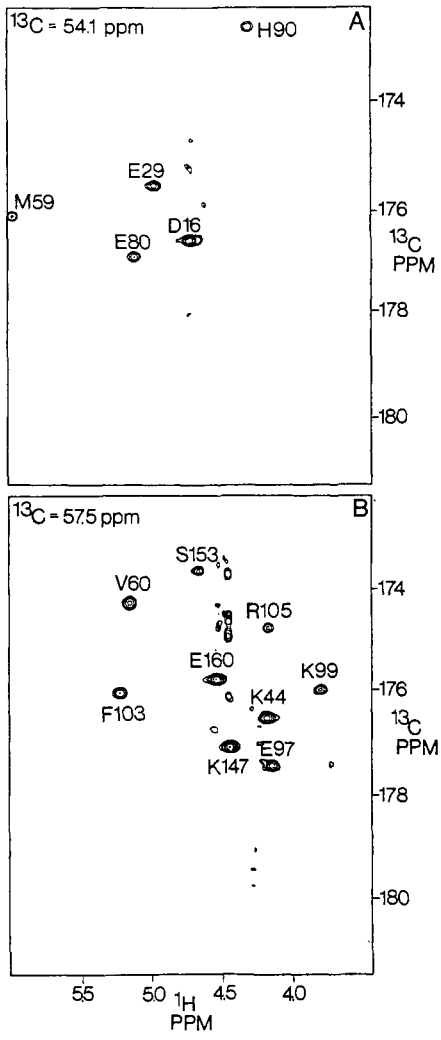

FIGURE 3: Representative planes from the 3D HCACO spectrum of III^{Glc}NC at ^{13}Cα chemical shifts of 54.1 ppm (A) and 57.5 ppm (B). Weak peaks at 4.67 ppm are due to residual HDO.

evolution period. Another alternative is to employ the recently developed 3D HN(CO)CA experiment, which correlates only HN, ^{15}N, and $^{13}C_{\alpha i-1}$ signals, and has the advantage that magnetization transfer is less sensitive to short ^{15}N T_2 values than the HNCA experiment (Bax & Ikura, 1991). For III^{Glc}, the few cases for which there were ambiguities did not pose an obstacle to making sequential assignments because of additional correlations obtained from experiments described below.

The ^{13}C′ signals, which are a key element of the sequential assignment process, were correlated to the previously determined intraresidue ^{13}Cα and Hα resonances through analysis of a 3D triple-resonance HCACO spectrum (Ikura et al., 1990c; Kay et al., 1990a) (Figure 3). This experiment links the Hα, ^{13}Cα, and ^{13}C′ spins of each residue through ^{13}Cα–Hα (140 Hz) and ^{13}Cα–^{13}C′ (55 Hz) couplings. For example, the ^{13}C′ signal of His-90 (172.6 ppm) was assigned by identifying the His-90 Hα cross peak (4.32 ppm) on the plane that most closely matched the His-90 ^{13}Cα resonance (53.9 ppm) (Figure 3A). Assignment of the ^{13}C′ signals was complicated by the similar chemical shifts of several ^{13}Cα–Hα pairs. For III^{Glc} there were 18 cases in which two residues had ^{13}Cα and Hα chemical shifts that were separated by 0.2 ppm or less and 0.02 ppm or less, respectively. In these cases the assignments could generally be narrowed to two or three possibilities and were subsequently determined during the sequential assignment process.

Assignment of Intraresidue Side-Chain ^{13}C and ^{1}H Signals to Specific Types of Amino Acids. In the case of small proteins (MW < 10 kDa), side-chain ^{1}H resonances are assigned by using a combination of COSY and TOCSY 2D spectra with the sample dissolved in D_2O. For a protein the size of III^{Glc}, however, these methods suffer a great loss in sensitivity from a decrease in magnetization transfer efficiency (shortened T_2 values) as well as severe cross-peak overlap. Moreover, III^{Glc} contains a large number of similar residues, which compounded the overlap problem. These difficulties were overcome by using a uniformly ^{15}N/^{13}C-labeled preparation of III^{Glc} (III^{Glc}NC) in conjunction with the recently developed 3D ^{13}C HCCH-COSY (Kay et al., 1990b; Bax et al., 1990a) and HCCH-TOCSY (Bax et al., 1990b; Clore et al., 1990) pulse sequences. These experiments rely on strong one-bond J_{CH} and J_{CC} rather than J_{HH} couplings to efficiently transfer magnetization among protons within a given residue either through a COSY-type mechanism involving neighboring ^{13}C nuclei (HCCH-COSY) or through a DIPSI-3 pulse sequence (Shaka et al., 1988) applied to ^{13}C magnetization (HCCH-TOCSY). In addition to greater sensitivity, these methods have the advantage that correlations are independent of conformation and therefore show more uniform intensity patterns for a given residue type. Furthermore, spreading the correlations into a third dimension (^{13}C chemical shift) significantly reduces the cross-peak overlap inherent in 2D spectra of proteins of this size and allows for complete ^{13}C side-chain assignments. The resulting planes (^{13}C frequency) are analogous to those of 2D COSY or TOCSY spectra for the ^{13}C-attached proton located on the diagonal, except that the cross peaks in a given plane are not symmetric with respect to the diagonal unless the pair of correlated protons are attached to the same carbon or to two different carbons that have degenerate chemical shifts.

For a given residue type, the initial spin system type assignments were obtained by searching for characteristic cross-peak patterns (Bax et al., 1990a,b; Clore et al., 1990) in the appropriate ^{13}Cα chemical shift ranges (planes) of both HCCH-COSY and HCCH-TOCSY spectra. This provided for the majority of ^{1}H side-chain type assignments. The spin system classifications were subsequently confirmed through identification of side-chain ^{13}C–^{1}H diagonal and associated cross peaks in appropriate planes of the spectra. The assignments are summarized in Table I.

The 16 Gly spin systems were identified by their distinctive ^{13}Cα chemical shifts (≈45 ppm) and by the symmetric Hα–Hα correlations produced in HCCH-COSY and HCCH-TOCSY spectra. The identifications were confirmed by comparison with signals observed in a ^{13}C HMQC spectrum of III^{Glc} labeled from [1,2-^{13}C]Gly (III^{Glc}SL).

The AMX spin systems (Wüthrich, 1986), of which there are 37 in III^{Glc}, were first identified in a HCCH-COSY spectrum. In Figure 4A, correlations are observed from the ^{13}Cα–Hα diagonal peaks of F41, F71, and S141 to their corresponding Hβ signals. Comparison with the HCCH-TOCSY spectrum (Figure 4B) showed no other correlations, indicating the spin systems were of the AMX type. This fact was confirmed by locating the ^{13}Cβ–Hβ diagonal and associated cross peaks in the HCCH-COSY spectrum. For example, in Figure 5A, the diagonal signals at 2.67 and 3.46 ppm are correlated with each other and with a signal at 4.34 ppm. Comparison with Figure 4A shows that these are the same three signals associated with F71, confirming that the spin system is of the AMX type and that F71 ^{13}Cβ resonates at 38.6 ppm. Similar correlations from the ^{13}Cβ–Hβ diagonal

Table I: ^{1}H, ^{15}N, and ^{13}C Chemical Shift Assignments for III^{Glc} (ppm) at 36.5 °C and pH 6.4

Ala	NH	^{15}N	$^{13}C'$	Hα	$^{13}C\alpha$	Hβ	$^{13}C\beta$	Ala	NH	^{15}N	$^{13}C'$	Hα	$^{13}C\alpha$	Hβ	$^{13}C\beta$
A24	8.51	125.0	177.1	4.02	50.9	1.41	18.1	A42	8.63	121.7	179.8	4.38	55.6	1.65	18.8
A51	8.22	119.5	175.3	5.24	50.0	0.80	22.1	A61	8.52	120.7	177.8	4.35	50.0	1.45	18.2
A76	6.48	117.9	175.1	4.83	49.4	0.22	23.0	A107	7.52	121.6	173.9	4.65	51.2	1.41	20.8
A131	8.90	121.2	178.9	4.64	51.6	1.38	19.2								

Arg	NH	^{15}N	$^{13}C'$	Hα	$^{13}C\alpha$	Hβ	$^{13}C\beta$	Hγ	$^{13}C\gamma$	Hδ	$^{13}C\delta$
R105	9.05	127.3	174.8	4.20	57.9					3.23, 3.47	43.7
R112	8.64	125.7	176.7	4.97	55.8	1.85, 1.90	29.6	1.75, 1.75	26.9	3.23, 3.23	42.5
R165	9.23	125.1	174.5	5.32	55.3	1.62, 1.68	33.3	1.55, 1.59	29.4	3.18, 3.18	43.3

Asn	NH	^{15}N	$^{13}C'$	Hα	$^{13}C\alpha$	Hβ	$^{13}C\beta$	Hγ	$^{15}N\gamma$	$^{13}C\gamma$
N32	8.43	121.6	177.3	4.72	53.7	2.76, 3.25	37.5	6.94, 7.76	114.0	177.1
N57			173.7	3.95	52.4	2.56, 3.11	39.9	6.64, 7.36	111.4	178.1
N74	8.46	112.5	170.5	4.28	55.0	2.77, 3.00	36.9	7.01, 8.01	114.6	176.9
N142	8.51	121.0	176.0	5.19	51.9	2.66, 2.85	36.3	6.84, 7.62	109.4	178.8

Asp	NH	^{15}N	$^{13}C'$	Hα	$^{13}C\alpha$	Hβ	$^{13}C\beta$	Asp	NH	^{15}N	$^{13}C'$	Hα	$^{13}C\alpha$	Hβ	$^{13}C\beta$
D4[a]	7.88	120.2	176.0	4.48	56.1	2.62, 2.75	41.3	D12	8.34	122.7	176.1	4.68	54.6	2.65, 2.73	41.3
D13	8.27	120.4	176.5	4.55	54.6	2.68, 2.68	41.0	D16	8.34	121.2	176.7	4.73	54.3	2.67, 2.77	
D35	7.68	116.5	176.7	4.73	54.4	2.69, 2.75		D38	8.10	121.6	177.3	4.74	54.8	2.87, 2.74	44.6
D48	7.39	116.3	175.0	5.28	51.0	2.64, 2.91	43.9	D64	8.30	119.7	177.6	4.98	53.5	2.65, 2.78	40.8
D82	8.79	125.3	176.8	4.57	57.2	2.74, 2.82	39.7	D94	9.61	122.7	176.5	4.65	56.4	2.86, 3.22	38.8
D117	8.47	123.1	176.8	4.65	55.1	2.59, 2.77	40.4	D123	8.12	121.7	174.9	4.68	51.5	2.30, 2.90	40.8
D144	8.74	117.2	177.3	4.48	56.3	2.69, 2.76	40.0								

Glu	NH	^{15}N	$^{13}C'$	Hα	$^{13}C\alpha$	Hβ	$^{13}C\beta$	Hγ	$^{13}C\gamma$
E21	8.76	125.9	174.3	4.88	55.6	1.85, 2.02	31.9	2.03, 2.33	37.9
E29	7.88	122.4	175.6	4.98	54.3	1.91, 1.95	33.0	2.20, 2.25	35.6
E34	9.09	117.5	176.8	4.23	59.3	1.92, 2.11		2.34, 2.69	37.4
E43	8.05	111.2	176.3	4.37	55.7	1.98, 2.31	28.1	2.21, 2.39	37.1
E72	9.38	122.3	177.2	3.99	60.0	2.16, 2.23	29.6	2.42, 2.42	36.3
E80	8.37	126.7	177.0	5.12	53.9	1.98, 2.05	31.3	2.11, 2.31	36.0
E86	8.98	129.5	174.7	5.10	55.2	1.84, 1.99	31.4	2.05, 2.18	36.7
E97	7.79	119.9	177.4	4.18	57.8	2.17, 2.21	29.3	2.36, 2.45	36.3
E101	7.66	124.5	174.2	4.08	58.2	2.02, 2.09	29.7	2.20, 2.35	36.3
E108	7.59	113.3	176.5	4.67	53.6	1.78, 2.04	33.0	2.32, 2.32	36.0
E109	8.67	120.2	178.0	3.72	59.1	2.01, 2.01	29.7	2.27, 2.37	38.0
E121	9.12	125.7	174.8	4.91	55.2	2.09, 2.43		2.17, 2.21	37.0
E128	9.32	117.9	178.9	3.94	59.5	2.00, 2.12	29.6	2.24, 2.55	37.9
E129	7.24	116.4	178.3	4.27	58.5	2.17, 2.24	30.3	2.17, 2.37	36.2
E145	7.91	116.3	175.7	4.44	56.1	2.08, 2.35	30.3	2.30, 2.44	36.9
E148	7.94	117.5	173.1	4.52	56.2	1.91, 1.91	34.0	2.08, 2.17	36.4
E160	7.90	117.9	175.8	4.57	57.5	1.68, 1.96	33.5	2.06, 2.33	35.9

Gln	NH	^{15}N	$^{13}C'$	Hα	$^{13}C\alpha$	Hβ	$^{13}C\beta$	Hγ	δNH	$^{15}N\delta$	$^{13}C\delta$
Q111	7.60	120.4	175.9	4.24	56.6	2.00, 2.35	31.1	2.39, 2.46	7.00, 7.43	111.4	180.2

Gly	NH	^{15}N	$^{13}C'$	Hα	$^{13}C\alpha$	Gly	NH	^{15}N	$^{13}C'$	Hα	$^{13}C\alpha$
G1				3.82, 3.82	43.5	G18	8.58	111.0	174.0	4.06, 4.06	45.6
G28	8.34	108.9	171.7	3.87, 5.16	45.9	G47	6.77	105.5	171.2	3.77, 4.65	44.8
G49	9.12	108.1	172.0	3.57, 5.21	46.2	G56	8.70	110.9	173.1	4.07, 4.31	45.0
G65	8.58	111.0	171.4	4.20, 4.46	46.9	G68	8.73	119.5	172.7	3.61, 4.22	46.0
G84	7.90	109.9	174.5	3.90, 4.17	46.1	G92	7.02	120.1	169.9	3.45, 3.72	46.2
G100	9.03	106.5	175.1	4.27, 4.46	45.0	G102	8.20	107.8	173.0	3.44, 3.94	44.8
G110	8.26	112.5	173.7	3.77, 4.27	45.4	G116	8.73	112.6	174.4	3.30, 4.64	44.5
G154	8.97	109.5	173.3	3.91, 4.47	44.5	G159	8.76	111.8	172.6	3.14, 4.11	46.2

His	NH	^{15}N	$^{13}C'$	Hα	$^{13}C\alpha$	Hβ	$^{13}C\beta$	His	NH	^{15}N	$^{13}C'$	Hα	$^{13}C\alpha$	Hβ
H75	6.89	106.7	172.4	3.63	55.2	1.25, 2.70	32.3	H90	7.54	126.4	172.6	4.33	53.9	1.94, 2.46

Ile	NH	^{15}N	$^{13}C'$	Hα	$^{13}C\alpha$	Hβ	$^{13}C\beta$	Hγ	$^{13}C\gamma$	$H\gamma_m$	$^{13}C\gamma_m$	Hδ	$^{13}C\delta$
I20	9.15	126.8	174.8	4.31	60.8	1.68	40.9	1.12, 1.59		0.83	17.2	0.85	14.2
I22	8.78	123.5	174.7	4.08	58.6	2.19	36.3	1.07, 1.44	26.6	0.71	17.9	0.59	10.3
I23	8.62	131.4	174.4	4.17	58.2	1.84	36.0	1.73, 1.90		0.57	18.0	0.57	8.7
I30	8.55	125.0	175.9	4.46	63.7	1.93	38.2	0.74, 1.82		1.14	17.4	0.66	
I33	9.31	126.7	176.2	3.87	62.8	1.63	39.0	1.29, 1.34	29.9	1.02	18.1	0.73	14.6
I45	7.59	118.6	178.7	3.75	63.9	2.03	37.2	1.23, 1.50	28.5	0.84	16.8	0.80	11.8
I50	8.26	113.3	173.2	4.91	57.9	2.29	43.4	1.34, 1.11	26.6	1.06	21.3	0.73	15.4
I52	8.11	119.5	175.5	4.75	59.2	1.29	42.4	1.33, 1.44		0.40	17.1	0.84	14.3
I67	8.82	127.7	176.3	4.18	61.2	2.33	36.5	1.43, 1.54	27.4	0.99	18.0	0.72	13.0
I70	9.40	124.2	176.1	4.58	61.9	1.55	39.8			1.15	17.4	0.61	13.5
I79	9.03	120.1	171.6	5.05	59.2	1.92	42.0	1.54, 1.56		0.91	16.2	0.86	16.4
I93	6.95	111.7	176.3	4.78	57.2	1.75	39.2	1.43, 1.59		1.03	18.3	0.73	10.7
I106	8.31	127.8	176.4	4.30	60.1	1.55	37.5	1.25, 1.25		0.82	17.1	0.62	8.7
I120	7.68	120.4	174.7	4.98	59.7	1.67	46.5			1.36	19.2	0.73	13.2
I140	8.98	124.7	175.8	4.72	60.4	2.25	37.6	1.36, 1.40	30.2	0.99	19.8	0.92	14.7
I146	7.41	116.6	175.4	4.42	59.5	2.17	38.8	1.48, 1.63	27.4	0.87	18.7	0.82	
I150	9.31	128.1	174.8	4.31	60.7	1.94	39.2	1.18, 1.43		0.84	17.5	0.78	

Table I (Continued)

Ile	NH	^{15}N	^{13}C′	Hα	^{13}Cα	Hβ	^{13}Cβ	Hγ	^{13}Cγ	Hγ$_m$	^{13}Cγ$_m$	Hδ	^{13}Cδ
I164	7.22	118.8	174.6	4.95	59.7	1.33	46.3			0.85	19.3	0.85	14.1
I166	9.26	122.4	175.2	5.08	59.1	1.84	42.6	1.13, 1.53	28.1	0.92	18.4	0.85	15.1

Leu	NH	^{15}N	^{13}C′	Hα	^{13}Cα	Hβ	^{13}Cβ	Hγ	^{13}Cγ	Hδ	^{13}Cδ	Hδ	^{13}Cδ
L2			177.6	4.14	56.5	1.27, 1.40	42.4	1.40	26.8	0.74	24.4	0.78	
L6	8.00	120.5			56.9								
L9	8.09	123.3	177.4	4.44	55.5	1.65, 1.65	42.4	1.65	27.0	0.90	24.0	0.94	24.6
L26	7.25	114.2	174.4	4.91	55.3	1.84, 2.43	44.9	1.94	28.1	1.00	27.8	1.05	28.1
L87	8.99	123.8	175.3	5.67	53.6	1.39, 1.59	46.1	1.60	28.4	0.71	27.2	0.78	27.2
L98	7.60	117.4	179.3	4.36	55.5	2.06, 2.18	40.6	1.79	28.4	0.87	23.6	0.98	26.0
L124	8.84	124.5	174.3	4.42	59.6	1.99, 2.26	38.9	1.82	27.0	1.15	25.9	1.28	23.3
L126	6.93	118.1	179.1	4.12	58.0	1.62, 1.68	42.5	1.51	27.2	0.76	25.0	0.89	24.8
L127	8.04	121.1	179.2	3.85	58.0	1.23, 1.92	42.2	1.52	27.6	0.63	26.6	−0.07	23.9
L135	7.91	121.6	175.9	3.88	56.6	1.58, 1.61	43.0	1.59	26.9	0.76	24.0	0.82	25.7
L149	8.62	126.4	174.6	4.79	55.0	1.43, 1.75	44.2	1.46	27.9	0.78	26.3	0.89	27.7
L152	7.59	123.8	173.8	4.64	53.8	1.58, 1.73	39.3	1.44	28.1	0.65	24.5	0.73	22.5

Lys	NH	^{15}N	^{13}C′	Hα	^{13}Cα	Hβ	^{13}Cβ	Hγ	^{13}Cγ	Hδ	^{13}Cδ	Hε	^{13}Cε
K5[a]	8.08	120.2											
K7[a]	8.03	120.8		4.23	55.7								
K14	8.16	120.8	176.7	4.32	56.3	1.80, 1.88	32.8	1.44, 1.44	24.4	1.69, 1.69	29.0	3.02, 3.02	
K15	8.15	121.6	176.3	4.37	56.5	1.80, 1.88	33.1	1.46, 1.46	24.2	1.71, 1.71	29.0	3.02, 3.02	
K44	8.02	114.8	176.5	4.21	57.5	1.92, 2.12		1.26, 1.67		1.52, 1.52		2.89, 2.89	42.5
K53	9.29	130.6	175.1	4.70	52.8	1.53, 1.99	32.4	1.31, 1.35		1.60, 1.60	28.9	2.96, 2.96	41.9
K58	7.03	113.6	174.8	4.91	55.7	1.69, 1.91	35.0			1.65, 1.65	29.3	2.82, 2.96	42.1
K69	7.80	122.2	176.1	4.66	54.8	1.67, 1.67	35.3	1.02, 1.24	24.5	1.44, 1.51	28.7	2.52, 2.52	41.7
K99	8.21	114.7	176.0	3.84	57.8	2.06, 2.11	29.6	1.45, 1.45		1.78, 1.78	29.1	3.06, 3.06	42.3
K104	9.11	121.7	174.9	4.69	55.4	1.72, 1.75	35.9	1.23, 1.42	24.6	1.68, 1.68	29.2	2.91, 2.91	41.9
K114	8.69	122.8	176.2	5.06	53.1	1.72, 1.77	35.0	1.43, 1.47	24.1	1.72, 1.72	28.7	3.05, 3.05	41.9
K130	8.01	115.2	177.3	4.35	58.3	1.66, 1.66	35.7			1.55, 1.59	29.0	2.92, 2.92	41.9
K132	9.76	124.5	177.8	4.00	59.6	1.84, 2.01	32.4	1.41, 1.65	25.1	1.79, 1.79	29.4	3.07, 3.07	41.9
K147	8.68	123.3	177.1	4.48	57.7	1.63, 1.83	33.6	1.41, 1.51	25.0	1.60, 1.65	28.9	3.00, 3.00	41.9
K151	8.71	127.4	176.0	4.29	56.9	1.78, 1.86	32.8	1.46, 1.46	24.6	1.69, 1.69	29.0	3.00, 3.00	41.9
K167	8.51	123.4	175.2	5.03	55.2	1.63, 1.92	35.0	1.45, 1.45	24.8	1.65, 1.65	29.0	2.86, 2.93	41.9
K168	8.62	129.7	179.6	4.32	58.1	1.82, 1.87	34.6	1.48, 1.66		1.69, 1.69	29.0	2.99, 3.02	41.5

Met	NH	^{15}N	^{13}C′	Hα	^{13}Cα	Hβ	^{13}Cβ	Hγ	^{13}Cγ
M59	9.52	119.4	176.3	5.95	54.4	2.23, 2.38	38.1	2.79, 2.79	33.1
M143	7.74	117.3	178.5	4.43	55.7			2.73, 2.85	31.7

Phe	NH	^{15}N	^{13}C′	Hα	^{13}Cα	Hβ	^{13}Cβ	2,6 H	3,5 H	4 H
F3	8.36	117.6		4.60	57.9	2.99, 3.20	38.9	7.26		
F41	7.34	115.8	178.4	4.68	59.6	2.68, 2.84	40.0	7.07	6.88	6.46
F71	8.17	126.5	178.3	4.34	59.2	2.67, 3.46	38.6	7.35	7.46	7.30
F77	8.53	114.5	171.5	5.59	55.6	3.02, 3.21	42.6	6.94	7.07	
F88	9.32	123.0	172.6	5.21	55.1	2.81, 2.98	41.8	7.04		
F91	8.92	126.7	176.2	4.55	58.5	2.78, 3.31	38.9	6.86	6.27	6.53
F103	7.59	115.4	176.0	5.23	57.5	2.72, 3.08	44.2	6.87	6.61	6.80
F122	7.78	117.0	173.4	5.60	54.9	2.28, 2.38	42.5	6.58	7.31	7.40

Pro	^{15}N	^{13}C′	Hα	^{13}Cα	Hβ	^{13}Cβ	Hγ	^{13}Cγ	Hδ	^{13}Cδ
P25		174.3	4.70	62.6	2.32, 2.54		1.94, 1.94		3.62, 4.20	50.9
P37	128.7	174.5	4.77	63.1	1.90, 2.44		1.94, 2.20		3.44, 3.81	51.1
P54	126.5	177.8	5.27	63.7	2.07, 2.37	34.5	1.78, 1.97	27.7	3.44, 4.35	52.5
P62	130.3	174.5	4.71	63.1	2.31, 2.36		1.77, 1.88		3.99, 4.61	50.7
P125	136.1	180.1	4.34	66.4	1.86, 2.33		2.17		3.82, 4.20	49.7
P137		173.7	4.28	62.6	1.13, 1.60	34.9			3.54, 4.33	51.3
P162	125.4	175.5	4.76	63.6	1.70, 1.96		1.88, 2.05		3.82, 4.16	50.9

Ser	NH	^{15}N	^{13}C′	Hα	^{13}Cα	Hβ	^{13}Cβ	Ser	NH	^{15}N	^{13}C′	Hα	^{13}Cα	Hβ	^{13}Cβ
S8[a]	8.05	115.5		4.43	58.6	3.88, 3.88	63.6	S11	8.23	118.9	174.4	4.48	58.2	3.84, 3.93	63.8
S27	8.47	115.2	173.9	4.69	58.1	3.69, 4.10	65.1	S78	9.35	114.6	174.2	5.90	55.4	3.90, 4.14	67.1
S81	9.65	123.8	176.2	5.03	58.0	3.87, 4.57	64.8	S83			174.4	4.48	57.0	3.95, 4.12	63.6
S133	7.01	105.6	174.3	4.48	56.9	4.05, 3.16	64.8	S141	8.79	119.6	175.6	4.80	59.0	3.61, 3.86	63.9
S153	7.56	108.7	173.7	4.67	57.8	3.77, 3.85	66.3	S155	8.31	115.0	175.7	5.02	58.5	3.79, 3.93	63.8

Thr	NH	^{15}N	^{13}C′	Hα	^{13}Cα	Hβ	^{13}Cβ	Hγ	^{13}Cγ
T17	8.17	114.2	175.5	4.36	62.2	4.36	69.8	1.26	21.6
T19	7.90	114.9	174.3	4.84	62.2	4.02	70.4	1.12	21.9
T55	7.94	107.9	174.9	4.52	61.0	4.42	70.8	1.19	21.8
T66	8.29	117.1	175.0	5.09	61.2	3.86	71.2	1.06	21.0
T73	7.42	103.4	173.7	4.19	62.4	4.95	67.2	1.30	22.2
T95	7.95	108.9	178.3	3.84	63.3	3.74	67.4	1.53	25.8
T118	8.81	119.5	173.0	3.78	66.1	3.98	68.5	1.16	24.0
T134	8.29	114.0	172.8	3.96	61.1	4.25	68.2	1.14	22.2
T136	8.19	116.6	173.9	5.02	60.8	3.96	72.3	0.86	19.2
T157	9.19	120.8	173.7	4.53	62.0	3.88	70.3	1.22	21.8
T161	7.76	116.6	172.7	4.60	61.9	3.86	70.7	1.65	23.2

Table I (Continued)

Val	NH	^{15}N	$^{13}C'$	Hα	$^{13}C\alpha$	Hβ	$^{13}C\beta$	Hγ	$^{13}C\gamma$	Hγ	$^{13}C\gamma$
V10	7.93	119.2	176.1	4.19	62.3	2.11	32.8	0.95	20.0	0.95	20.3
V31	9.32	128.6	174.6	4.40	60.0	1.86	35.4	0.74	21.0	0.98	20.5
V36	7.50	120.5	176.6	4.01	60.2	2.24	31.7	0.85	22.4	0.94	23.0
V39	8.60	125.9	176.2	3.95	65.8	2.17	32.0	0.99	20.5	0.99	18.8
V40	7.99	118.2	177.7	3.65	65.8	1.76	30.8	0.66	21.6	0.48	20.9
V46	7.40	112.7	174.5	4.07	62.1	2.07	31.5	0.61	20.0	0.68	21.3
V60	9.99	118.0	174.3	5.17	57.6	1.79	34.6	0.74	20.7	0.74	19.0
V63	7.19	109.7	172.6	4.46	58.4	2.22	36.3	0.56	19.2	0.89	23.6
V85	8.14	120.3	173.7	4.17	62.2	1.92	33.1	0.78	21.8	0.91	22.6
V89	8.00	126.2	173.3	4.37	60.6	0.78	32.7	0.61	21.7	0.45	20.3
V96	8.37	123.8	177.8	3.67	64.7	2.11	31.3	1.13	21.7	0.94	20.2
V113	9.14	118.2	175.0	4.89	59.0	2.25	36.2	0.87	22.3	0.74	19.2
V115	8.26	118.5	178.0	3.26	64.2	1.79	31.7	0.79	20.7	0.86	22.0
V119	9.04	124.6	175.9	4.10	63.6	1.11	33.8	−0.03	19.4	0.38	20.2
V138	8.77	124.4	174.5	4.33	62.1	2.04	32.8	0.63	20.0	0.82	20.7
V139	8.64	116.9	174.3	4.85	59.0	1.84	36.3	0.72	21.8	0.92	20.3
V156	9.28	116.3	175.5	4.87	59.1	1.91	36.3	0.82	23.2	0.81	
V158	8.89	129.4	173.9	3.31	62.0	2.55	31.7	0.94	24.8	1.00	18.8
V163	8.96	109.7	173.8	4.60	61.0	2.15	33.2	0.72	18.0	0.98	24.0

[a] Tentative assignment.

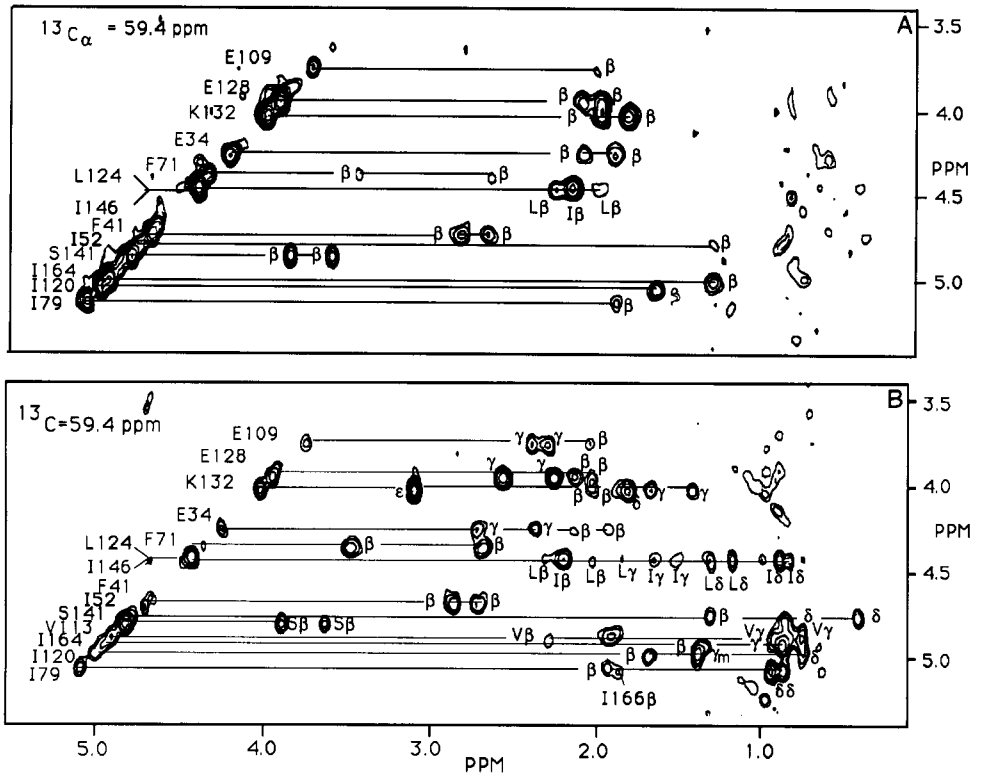

FIGURE 4: Expansion of planes ($^{13}C\beta$ = 59.4 ppm) taken from HCCH-COSY (A) and HCCH-TOCSY (B) spectra of $III^{Glc}NC$. Correlations are seen from each ^{13}C-attached Hα proton (diagonal) to Hβ (HCCH-COSY) and to all other intraresidue ^1H signals (HCCH-TOCSY). Residue assignments are indicated along the diagonal.

signals for several Asx and Phe spin systems are shown in Figure 5A,B.

Following the method outlined above, we were able to identify all 37 AMX spin systems. From these, the 10 serine residues were identified on the basis of their downfield-shifted (62 ppm) $^{13}C\beta$ signals and through comparison of $^{13}C\alpha$ and $^{13}C\beta$ signals with those obtained in 2D ^{13}C HMQC spectra of $III^{Glc}SL$, which was partially labeled at all three ^{13}C serine positions as a result of cross labeling with [1,2-^{13}C]Gly. The eight Phe spin systems were identified in a similar manner through comparison of $^{13}C\beta$ shifts with those obtained from ^{13}C HMQC spectra of $III^{Glc}SL$ (labeled with [3-^{13}C]D,L-Phe) (supplementary material). Given these assignments, partial Phe ring proton assignments were obtained from Hβ-2,6H NOEs observed in a 2D ^{13}C HMQC-NOESY spectrum and correlations observed in homonuclear 2D DQF-COSY and TOCSY/HOHAHA spectra of $III^{Glc}SL$ (supplementary material). Finally, the four Asn residues were distinguished on the basis of Hβ–γNH NOEs observed in a 3D ^{15}N NOESY-HMQC spectrum of $III^{Glc}N$ (Pelton et al., 1991).

The 17 Glu, the single Gln, and the 2 Met spin systems were resolved in a similar manner. For example, comparison of the HCCH-COSY spectrum shown in Figure 4A with the HCCH-TOCSY spectrum shown in Figure 4B indicates that the degenerate Hβ signals of E-109 occur at 2.01 ppm, while the Hγ protons resonate at 2.27 and 2.37 ppm. The spin system classification was confirmed, and the $^{13}C\beta$ and $^{13}C\gamma$ signals were obtained through identification of $^{13}C\beta$–Hβ and $^{13}C\gamma$–Hγ diagonal and associated cross peaks in the appropriate planes of both spectra. Examples of such correlations are shown for

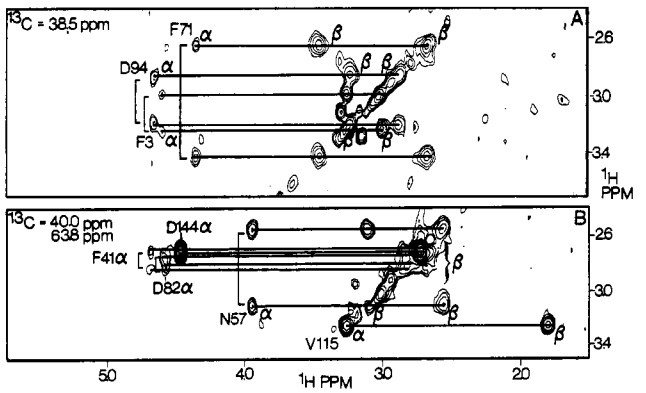

FIGURE 5: Expansion of planes from an HCCH-COSY spectrum of III^{Glc}NC corresponding to ^{13}Cβ chemical shifts of 38.5 ppm (A) and 40.0 ppm (B). Correlations are observed from ^{13}Cβ–Hβ diagonal to Hα signals of several AMX spin systems. Note that because of the extensive folding employed in the ^{13}C dimension (Bax et al., 1990), a correlation is also observed in this expansion from V115 ^{13}Cα (64.2 ppm)–Hα to its own Hβ proton.

several Glu residues in Figure 6. The single Gln spin system was identified on the basis of Hγ–δNH NOEs in a 3D ^{15}N NOESY-HMQC spectrum of III^{Glc}N.

III^{Glc} contains 68 residues that have at least one methyl group. Identification of the 7 Ala and 11 Thr spin systems was based on observation of strong ^{13}Cα–Hα to methyl proton (Ala Hβ, Thr Hγ) and reverse ^{13}C-methyl to Hα correlations (Figure 7A). Calculations that take into account effective Thr ^{13}C–^{13}C coupling constants (reduced due to ^{13}C chemical shift differences) and spin–spin relaxation times (T_2) have predicted that correlations to Thr Hβ protons will be weak or absent in HCCH-TOCSY spectra (Bax et al., 1990b). Thus, ^{13}Cα chemical shifts were initially used to distinguish between Ala ($\approx$ 52.9 ppm) and Thr ($\approx$ 61.9 ppm) spin systems (Howarth & Lilley, 1978). The type assignments were confirmed through identification of Thr ^{13}Cβ–Hβ signals and associated cross peaks to Hα and Hγ signals in HCCH-COSY spectra. Examples of such correlations are shown in Figure 7b, where it can be seen that the ^{13}Cβ–Hβ diagonal signals of T19 and T55 correlate with their respective Hα and Hγ protons previously identified in Figure 7A.

Identification of the remaining methyl-containing residues (19 Val, 19 Ile, and 12 Leu) posed a particular assignment challenge because their disproportionate numbers and the similarities of their side-chain configurations make it difficult to distinguish among their similar connectivity patterns. Previous work has shown that the ^{13}Cα chemical shifts of Val and Ile in peptides (Levy & Nelson, 1972; Howarth & Lilley, 1978) and proteins (Wagner & Bruehwiler, 1986; Clore et al., 1990) are similar (58–63 ppm) whereas the large portion of Leu ^{13}Cα signals are shifted slightly upfield (55.6 ppm). Thus, we expected correlations for Val and Ile to occur on the same ^{13}Cα planes and for these to be separated in large part from Leu correlations. In addition, theoretical calculations (Clore et al., 1990) predict that Ile ^{13}Cα–Hα to Hγ correlations are weak, implying that the Ile cross-peak pattern derived from ^{13}Cα–Hα signals would appear similar to those of Val. With these considerations in mind, we searched in the Ile–Val and Leu ^{13}Cα chemical shift regions of the HCCH-TOCSY spectrum for spin systems that contained correlations to a pair of methyl groups. Examples of such correlations are shown in Figure 4A,B for V113 and several Ile residues, as well as

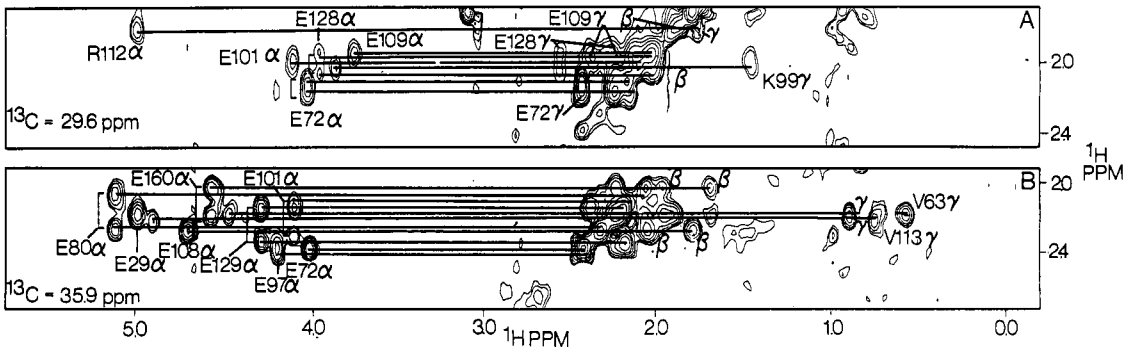

FIGURE 6: Glutamic acid/glutamine side-chain connectivities. Shown are correlations from ^{13}Cβ–Hβ diagonal peaks in a HCCH-COSY spectrum (^{13}Cβ = 29.6 ppm) (A) and from ^{13}Cγ–Hγ diagonal peaks in a HCCH-TOCSY spectrum (^{13}Cγ = 35.9 ppm) (B).

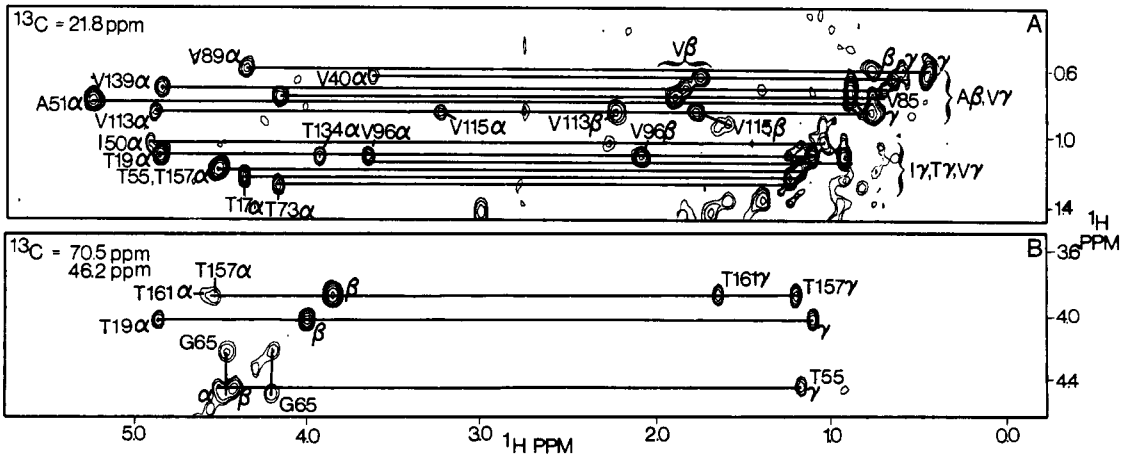

FIGURE 7: Identification of Ala, Thr and Val spin systems. Portion of a HCCH-TOCSY spectrum (^{13}C = 21.8 ppm) showing correlations from ^{13}C methyl to Thr and Val Hα resonances (A) and portion of a HCCH-COSY spectrum (^{13}Cβ = 70.5 ppm) showing correlations from Thr ^{13}Cβ-Hβ to Hα and Hγ signals (B). Note that the ^{13}Cα (46.9 ppm) signal of Gly 65 occurs on the same plane as several Thr ^{13}Cβ signals due to folding in the ^{13}C dimension.

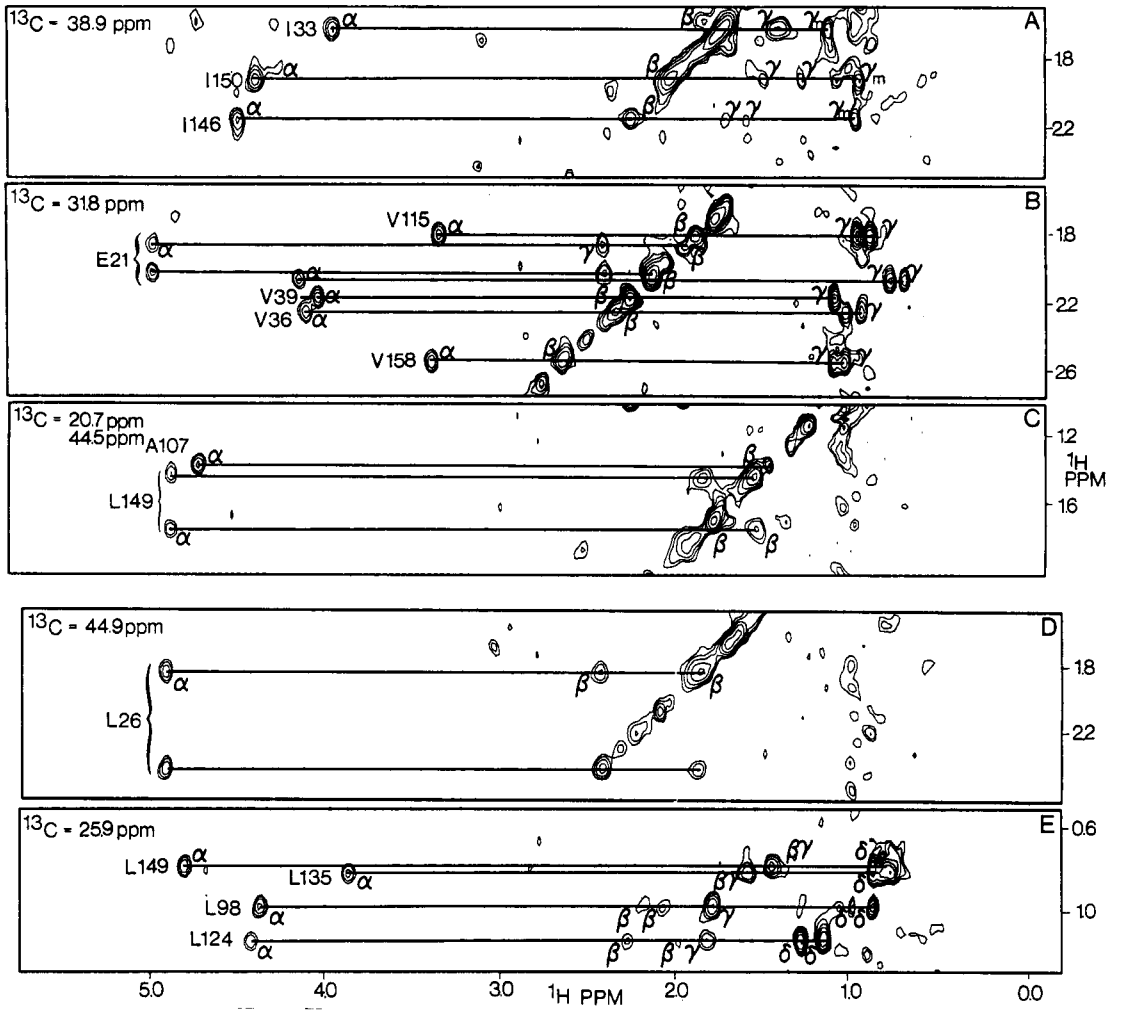

FIGURE 8: Portions of HCCH-COSY and HCCH-TOCSY spectra of III^{Glc}NC used to assign Val, Ile, and Leu spin systems. Correlations observed in an HCCH-COSY spectrum from Ile ($^{13}C\beta$ = 38.9 ppm) (A), Val (31.8 ppm) (B), Leu (44.5 ppm) (C), (44.9 ppm) (D), and in a HCCH-TOCSY spectrum from Leu $^{13}C\gamma$-Hγ signals (25.9 ppm) (E). Because of folding in the ^{13}C dimension, the $^{13}C\beta$ signal of A107 (20.8 ppm) occurs on the same plane as Leu-149 (44.8 ppm) (C).

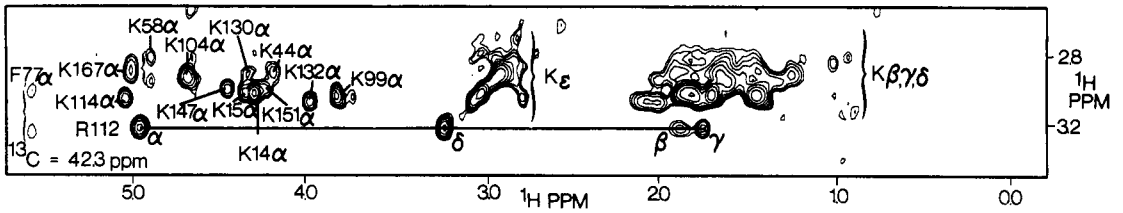

FIGURE 9: Portion of a plane from an HCCH-TOCSY spectrum of III^{Glc}NC ($^{13}C\epsilon$ = 42.3 ppm) showing correlations from Lys $^{13}C\epsilon$–Hϵ to Hα and other side-chain signals. Note the significant chemical shift degeneracy of the Hβ, Hγ, and Hδ resonances.

Leu 124. Note that the expected Ile Hγ cross peaks of I79, I120, and I164 are missing and that the Ile and Val spin systems could not be resolved on the basis of these data alone. Once the majority of spin systems with a pair of methyl groups were obtained and the Hβ signals were assigned from the corresponding planes of the HCCH-COSY spectrum, a search was conducted for correlations from the $^{13}C\beta$–Hβ signals. As can be seen in Figure 8A,B, the Ile and Val spin systems can be distinguished by the presence or absence of Hγ signals, respectively. Moreover, the Leu spin systems can be resolved from the other two by the presence of the characteristic $^{13}C\beta$H doublet (Figure 8C,D). The other ^{13}C signals were assigned by searching in the appropriate planes. For example, correlations from the Leu $^{13}C\delta$–Hδ protons, which provided for assignment of $^{13}C\delta$ methyl signals, are shown in Figure 8E.

Assignment of the 17 Lys and 3 Arg residues also posed a challenge because, as previously noted (Wüthrich, 1986), the side-chain ^{1}H and ^{13}C signals are generally poorly resolved. Correlations from 12 Lys $^{13}C\epsilon$–Hϵ and one Arg $^{13}C\delta$–Hδ pair are shown in the HCCH-TOCSY spectrum of Figure 9. Although most of the Lys Hϵ have similar chemical shifts, we were able to resolve all of the Hα signals, which showed good chemical shift dispersion. Given the Hα and Hϵ assignments, a search was made for $^{13}C\alpha$–Hα and other side-chain ^{13}C–^{1}H signals in both the HCCH-COSY and HCCH-TOCSY spectra (Figure 4).

Finally, although Arg and Pro have identical spin systems, these residues were easily distinguishable in HCCH spectra. In general, Pro $^{13}C\alpha$ signals ($\approx$ 64 ppm) resonate considerably upfield of Arg $^{13}C\alpha$ signals ($\approx$ 55 ppm) and therefore appear on different planes of the 3D spectrum. In addition, Pro $^{13}C\beta$–Hβ to Hγ cross peaks are usually significantly less intense than those of Arg due to restricted motion of the side-chain atoms (shorter T_2s) (Clore et al., 1990). The proline

spin system classifications were subsequently confirmed through comparison with Pro $^{13}C\alpha$–Hα signals obtained from a ^{13}C HMQC spectrum of III^{Glc}SL (labeled with [2-^{13}C]Pro) (supplementary material).

After identification of virtually all of the spin systems, as described above, we completed the intraresidue assignments by matching the backbone (^{15}N, NH, $^{13}C\alpha$, Hα, $^{13}C'$) and side-chain ($^{13}C\alpha$, Hα) signals through comparison of $^{13}C\alpha$ and Hα resonances obtained from the HOHAHA-HMQC and HNCA experiments with those obtained from HCCH spectra. This process was complicated by several factors. For example, 3 ^{15}N–^{1}H and 18 $^{13}C\alpha$–Hα pairs had ^{15}N or $^{13}C\alpha$ chemical shift differences of 0.2 ppm or less and ^{1}H chemical shift differences of 0.02 ppm or less and were not readily resolved in 3D spectra. In addition, Hα signals for 15% of the residues were not observed in the ^{15}N–^{1}H HOHAHA-HMQC spectrum due either to saturation by the DANTE presaturation pulse or because of small $^{3}J_{NHH\alpha}$ couplings. To resolve these ambiguities, we found it helpful to assign as many Hβ signals from the 3D ^{15}N HOHOHA-HMQC spectrum as possible for comparison with those determined from the HCCH spectra.

Additional information on amino acid type assignments was derived from the specifically labeled sample (III^{Glc}SL) in which ^{15}N enrichment of Lys, Leu, Phe, and His were calculated to be 100%, 60%, 40%, and 27%, respectively. Examination of ^{15}N HSQC spectra of III^{Glc}SL and comparison with those of III^{Glc}N revealed that the Lys residues were well labeled (≈80%) but that incorporation of the remaining amino acids was lower than anticipated (20–30%). As a consequence, the ^{15}N–^{1}H signals of the Lys residues were easily identified, while the remaining ^{15}N–^{1}H correlations were classified only as belonging to either Leu, Phe, or His spin systems.

Combining the data derived from the triple-resonance experiments, the classification of virtually all of the side-chain spin systems using the HCCH data, and the information obtained from 2D ^{15}N HSQC and ^{13}C HMQC experiments on III^{Glc}SL, we were able to match backbone and side-chain signals for approximately 70% of the residues. In addition, we had identified the backbone ^{15}N, NH, $^{13}C\alpha$, Hα, and $^{13}C'$ signals, which were needed for determination of $^{13}C_{\alpha i,i-1}$, $^{13}C'_{i,i-1}$, and $^{15}N_{i,i+1}$ sequential linkages (see below) for 60% of the remaining residues. Although we were not initially able to match the backbone and side-chain atoms unambiguously in these cases for the reasons stated above, these linkages were subsequently determined during the sequential assignment process.

Sequential Assignments. In the first phase of the sequential assignment process, information about sequential connectivities was derived from 3D triple-resonance HNCA, HNCO, and HCA(CO)N spectra (Ikura et al., 1990c, 1991; Kay et al., 1990a). These experiments rely on single-bond J_{CN}, $J_{CC'}$, and $J_{C'N}$ couplings in combination with large ^{15}N and $^{13}C'$ T_2 values to transfer magnetization and correlate neighboring residues. As was noted previously, in the HNCA experiment, correlations are observed not only between NH, ^{15}N, and intraresidue $^{13}C\alpha$ signals but also to the $^{13}C\alpha$ of the preceding residue via the two-bond $^{15}N_i$–$^{13}C\alpha_{i-1}$ coupling (≈ 7 Hz). As can be seen in Figure 2 for residues L87–G100, the pair of correlations observed for most of the ^{15}N–^{1}H signals provides for one type of sequential connectivity. Using a mixing time of 22 ms, we were able to identify 80% of the possible $^{15}N_i$–$^{13}C\alpha_{i-1}$ correlations.

In the HNCO experiment (Ikura et al., 1990c; Kay et al., 1990a), each intraresidue ^{15}N–^{1}H pair is correlated with the $^{13}C'$ signal of the preceding amino acid, providing a second

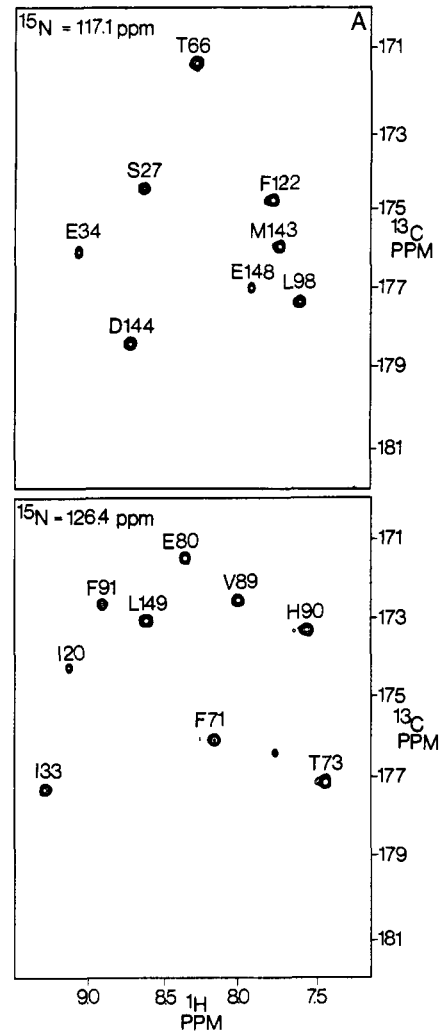

FIGURE 10: Representative planes taken from a 3D HNCO spectrum of III^{Glc}NC taken at ^{15}N chemical shifts of 117.1 ppm (A) and 126.5 ppm (B).

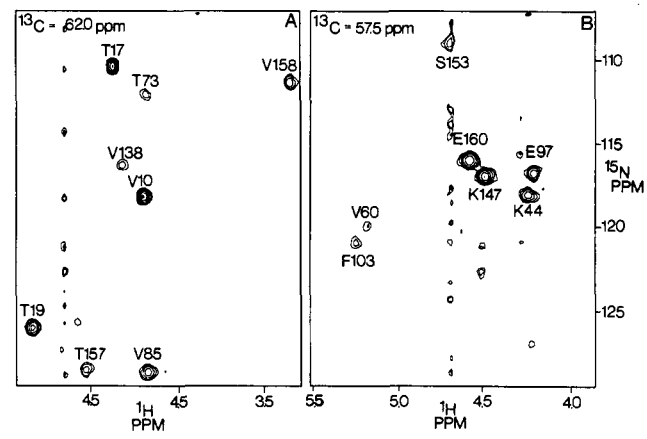

FIGURE 11: Representative planes taken from a 3D HCA(CO)N spectrum of III^{Glc}NC taken at $^{13}C\alpha$ chemical shifts of 62.0 ppm (A) and 57.5 ppm (B).

sequential connectivity. Slices taken from planes of the 3D spectrum are shown in Figure 10. Because of the excellent dispersion of the ^{15}N–^{1}H signals, we were able to match 95% of the amino acid spin systems with the $^{13}C'$ resonance of the preceding residue.

Finally, in the HCA(CO)N experiment (Ikura et al., 1990c; Kay et al., 1990a) each $^{13}C\alpha$–Hα pair is correlated with the ^{15}N signal of the following residue providing a third inde-

pendent sequential connectivity. Several planes from this 3D spectrum are shown in Figure 11. Note that because the spectrum is recorded in D_2O, the peaks are broadened in the ^{15}N dimension due to the J_{ND} coupling. We observed 90% of the possible $H\alpha$–$^{13}C\alpha$–$^{15}N_{i+1}$ correlations. However, not all of the correlations could be uniquely identified because several $^{13}C\alpha$–$H\alpha$ pairs had similar chemical shifts. In such cases there were at most two or three possible ways to assign the correlations. These were later resolved during the sequential assignment process.

At this point, we had obtained three types of sequential connectivities ($^{13}C\alpha_{i-1}$–$^{15}N_i$–NH_i; $^{13}C'_{i-1}$–$^{15}N_i$–NH_i; $^{15}N_{i+1}$–$^{13}C\alpha_i$–$H\alpha_i$) for 85% of the residues and had matched 70% of the ^{15}N–^1H correlations with their corresponding side-chain spin systems. The next phase of the assignment process involved the use of triple-resonance data along with the primary sequence to assign signals to particular amino acids in the sequence. The sequential assignments were started by selecting a residue in which the preceding $^{13}C\alpha$ (HNCA) and $^{13}C'$ (HNCO) signals were extremely upfield- or downfield-shifted. For example, the $^{13}C\alpha$ and $^{13}C'$ signals of the residue preceding an Ile (I93) occur at 46.2 and 169.9 ppm, respectively, which are characteristic of glycine. The glycine residue with these signals was identified (G92) and the sequential assignment was confirmed via the Gly–Ile $^{15}N_{i,i+1}$ correlation [HCA(CO)N]. Examination of the sequence revealed that this pair could be one of two Gly–Ile dipeptides (G92–I93 or G49–I50) and that the residue preceding Gly had to be either Asp or Phe with $^{13}C\alpha$ and $^{13}C'$ signals at 58.5 and 176.2 ppm, respectively. The $^{13}C\alpha$ and $^{13}C'$ resonances matched those of Phe-91, and consequently the Gly–Ile dipeptide was determined to be that of Gly-92–Ile-93. Groups of 5–10 sequential residues were assigned in a similar manner and were pieced together to yield virtually complete sequential assignments. In this approach to sequential assignment of amino acids, we utilized the triple-resonance sequential heteroatom connectivities, the amino acid type assignments, the primary sequence, and data correlating $^{13}C\alpha$ chemical shifts with amino acid types in peptides (Levy & Nelson, 1972; Howarth & Lilley, 1978) and proteins (Wagner & Bruehwiler, 1986; Clore et al., 1990; Spera & Bax, 1991).

The sequential assignment procedure depends critically on the reproducibility of ^{15}N and ^{13}C chemical shifts derived from the different triple-resonance experiments. In our experience, the reproducibility of $^{15}N_i$ and $^{15}N_{i+1}$ signals derived from HSQC (in H_2O) and HCA(CO)N spectra (in D_2O) [after 0.7 ppm was added to ^{15}N chemical shifts obtained from the HCA(CO)N data to account for a ^1H vs ^2H isotope shift] was ±0.1 ppm or better in 93% of the cases and better than ±0.2 ppm for all correlations. Similarly, the reproducibility of $^{13}C'$ chemical shifts derived from HCACO and HNCO spectra was ±0.05 ppm or better for 88% of the cases and better than ±0.2 ppm for all linkages. Matching the $^{13}C\alpha$ chemical shifts posed no problem because they were derived from intra- and interresidue connectivities observed in a single 3D spectrum.

In total, 132 $^{13}C\alpha_{i,i-1}$, 150 $^{13}C'_{i,i-1}$, and 144 $^{15}N_{i,i+1}$ linkages were established and used to sequentially assign the 168 residues of III^{Glc} (Figure 12). The assignments are summarized in Table I. Note in Figure 12 that the sequential linkages are interrupted at each of the seven prolines because they lack amide protons. This is also true for those amino acids (Gly-1, Leu-2, Asn-57, Ser-83) for which the amide proton has not been assigned. In these cases, the sequential assignments must rely on linkages from the following residue (i.e., $^{13}C\alpha_{i,i-1}$ and $^{13}C'_{i,i-1}$ linkages). Additional information confirming the correct proline assignments was obtained from analysis of 3D NOESY-HMQC spectra (Marion et al., 1989a; Kay et al., 1989; Ikura et al., 1990a). For all of the Pro residues except Pro-125, clear $d_{\alpha\delta}$ NOE connectivities were identified in a 3D ^{13}C NOESY-HMQC spectrum. For Pro-125, $d_{N\delta}$ NOEs were observed in a 3D ^{15}N NOESY-HMQC spectrum, confirming the sequential assignment. Furthermore, these data show that all seven Pro residues are in the trans conformation (Wüthrich, 1986).

Ambiguities can arise in the sequential assignment process when two or more residues have overlapping pairs of ^{15}N–^1H or $^{13}C\alpha$–^1H signals (Ikura et al., 1990). For III^{Glc}, 3 ^{15}N–^1H and 18 ^{13}C–^1H pairs had heteronuclear chemical shift differences of 0.2 or less, as well as ^1H chemical shift differences of 0.02 or less, and were therefore not readily distinguished in 3D spectra. We were able to resolve these ambiguities during the sequential assignment process with the aid of both $^{13}C'_{i,i-1}$ and $^{15}N_{i,i+1}$ sequential linkages and the primary sequence. In addition, ambiguities can arise if the $^{13}C'$ and ^{15}N signals of two or more residues are coincident. We are able to resolve the 13 pairs of these degeneracies with the aid of $^{13}C\alpha_{i,i-1}$ linkages obtained from the HNCA experiment.

The sequential assignments were checked against data obtained from the specifically labeled sample ($III^{Glc}SL$) in which $^{13}C'$ and ^{15}N double labels were incorporated (Torchia et al., 1989b; Ikura et al., 1990b). In this method, an ^{15}N-labeled amino acid that has a $^{13}C'$-labeled neighbor shows a characteristic splitting in the ^{15}N dimension of HSQC spectra due to the $^{13}C'$–^{15}N coupling (≈ 15 Hz). Analysis of a ^{15}N HSQC spectrum of $III^{Glc}{}_{SL}$ (supplementary material) showed that six Lys ^{15}N signals were doublets consistent with the present assignments. The observed intensities of the doublet components were unequal because the level of $^{13}C'$ incorporation for Leu and Ile were at most 60% and 40%, respectively, and because the downfield doublet signal coincides with the ^{15}N–^{12}C singlet (Ikura et al., 1990b). Doublets were also expected for Leu-2 (by Gly-1), Phe-3 (by Leu-2), Lys-7 (by Leu-6), Phe-71 (by Ile-70), and Leu-127 (by Leu 126) but were not observed because the cross peaks were particularly weak. Leu-2, Phe-3, and Lys-7 reside in the nonstructured N-terminal region of the protein, and it is highly likely they are reduced in intensity as the result of rapid exchange with solvent. Moreover, the Phe and Leu ^{15}N incorporation was less than expected; and thus, although each of the 8 Phe and 10 of the 12 Leu ^{15}N–^1H signals were identified (F3 and L6 at pH 5.5), the expected splittings were not clearly resolved because of the low signal-to-noise ratio. The modest levels of $^{13}C'$ enrichment of [1-^{13}C]Leu, and [1-^{13}C]Ile (ca. 50%) also contributed to the difficulty in observing the splittings.

Discussion

Using triple-resonance 3D NMR experiments in combination with 3D HCCH-COSY and HCCH-TOCSY spectra, we have sequentially assigned virtually all ^1H, ^{15}N, and ^{13}C signals of III^{Glc} (Table I). The fact that these experiments rely on J couplings to transfer magnetization between ^1H, ^{15}N, and ^{13}C nuclei made it possible to complete the assignments without reference to NOESY (through space) connectivities except in cases where distances are known to be short (for example, between aromatic ring protons and Gln δNH–$H\gamma$ protons). Thus, the assignments were made without reference to secondary structure and without the aid of a crystal structure. Moreover, only three samples, one uniformly ^{15}N enriched, one uniformly $^{15}N/^{13}C$ enriched, and one specifically labeled at several positions with ^{13}C and ^{15}N were required. The only substantial drawback to this method of assignment is that, at

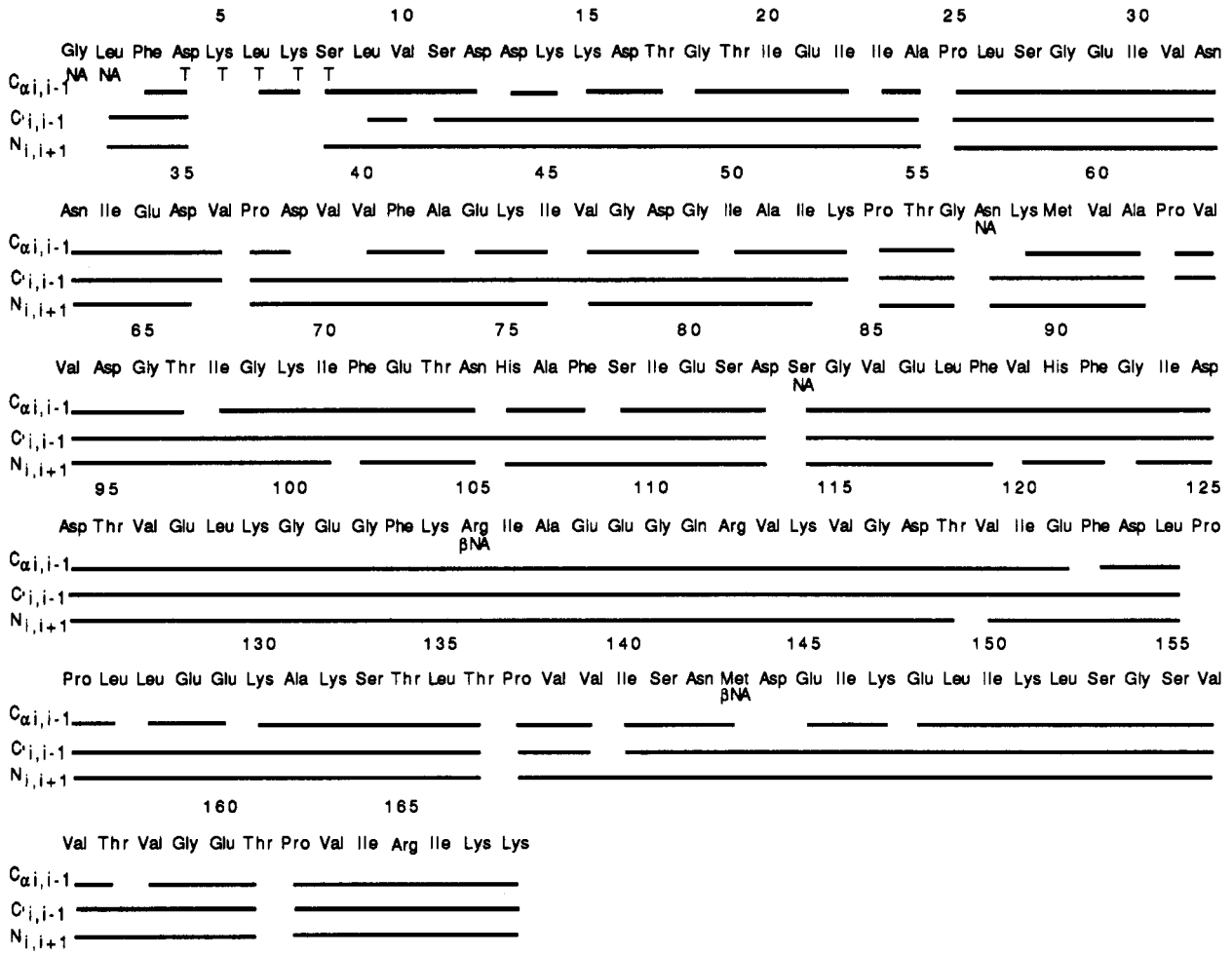

FIGURE 12: Sequential $^{13}C\alpha_{i,i-1}$, $^{13}C'_{i,i-1}$, and $^{15}N_{i,i+1}$ linkages used to assign the residues of III^{Glc}. Note that breaks in the connectivities occur at each of the seven Pro residues because they lack amide protons. The letter T denotes that the residue is tentatively assigned. The letters NA and βNA indicate that the amide NH or the Hβ protons, respectively, were not assigned. Note that Asn-32, Val-63, Pro-125, and Val-156 have been repeated on each side of the figure.

the present cost of [$^{13}C_6$]glucose, an efficient expression system must be available.

In total, we have assigned backbone signals for all residues except for the NH and ^{15}N of Gly-1, Leu-2, Asn-57, and Ser-83. In addition, we were able to assign 95% of the side-chain ^1H signals and 85% of the ^{13}C side-chain signals. With regard to the carbon assignments, the Pro $^{13}C\beta$ and $^{13}C\gamma$ as well as the Ile $^{13}C\gamma$ resonances proved difficult to assign mainly because the peaks were weak in both HCCH-COSY and HCCH-TOCSY spectra. In addition, the Lys $^{13}C\gamma$ resonances were particularly hard to resolve due to extensive overlap of the Hγ signals (Table I).

The assignment strategy used here paralleled more traditional methods (Wüthrich, 1986) in the sense that most spin systems were identified before attempting to sequentially assign particular amino acids. This allowed us to use the triple-resonance linkages, the primary sequence, and characteristic $^{13}C\alpha$ chemical shift ranges of individual amino acids to make sequential assignments. One could also make sequential backbone assignments relying primarily on the triple-resonance linkages and a small number of side-chain spin system identifications as was done for calmodulin (Ikura et al., 1990c, 1991). The backbone linkages, the primary sequence, and the HCCH spectra could then be used together to assign the remaining spin systems and confirm that the correct sequential assignments had been made. We feel both approaches work equally well and that the correct strategy to use in a particular situation will depend on the quality and extent of available interresidue linkages. Moreover, including primary sequence data and characteristic ^{13}C chemical shift ranges of amino acids into computer algorithms designed to correlate triple-resonance linkages (Ikura et al., 1990c) should aid in the goal of completely automating backbone assignments for proteins of this size.

The spread of ^{13}C chemical shifts for the various types of residues of III^{Glc} (Table I) is considerably larger than those found in unstructured peptides (Levy & Nelson, 1972; Howarth & Lilley, 1978) and similar to the dispersion of shifts observed in native proteins (Clore et al., 1990; Wagner & Bruehwiler, 1986; Spera & Bax, 1991). There is considerable interest in correlating ^{13}C chemical shifts with protein sequence and secondary structure. For example, it has been noted (Torchia et al., 1975; Clore et al., 1990) that the $^{13}C\alpha$ chemical shifts of amino acids that precede Pro residues are upfield shifted from their random coil values. For III^{Glc}, three amino acids that precede Pro residues (Lys-53, Ala-61, and Thr-136) have $^{13}C\alpha$ chemical shifts that are the most upfield of their respective classes, while a fourth (Thr-161) is on the upfield side of the Thr range. In contrast, the $^{13}C\alpha$ chemical shifts of Ala-24 and Val-36 (which precede Pro-25 and Pro-37) occur near the middle of their respective ranges, while that of Leu-124 (which precedes Pro-125) is the most downfield-shifted of the 12 Leu residues. Hence, other factors such as secondary structure must also influence ^{13}C chemical shifts. In this regard, several workers (Saitô & Ando 1989, Spera & Bax, 1991) have noted that $^{13}C'$, $^{13}C\alpha$, and $^{13}C\beta$ chemical

shifts are sensitive to conformation. For example, Spera and Bax (1991) have correlated differences in $^{13}C\alpha$ and $^{13}C\beta$ chemical shifts from random coil values with ϕ and ψ angles for four proteins. They concluded that $^{13}C\alpha$ signals shift downfield (3 ppm) or upfield (2 ppm) and $^{13}C\beta$ signals show no deviation or shift upfield (3 ppm) depending on whether the residues are found in α-helices or in antiparallel β-sheets, respectively. For III^{Glc}, four regions, HI (residues Glu-34–Gly-42), HII (Asp-94–Phe-103), HIII (Pro-125–Leu-135), and HIV (Ser-141–Glu-148), were characterized as containing helical segments on the basis of d_{NN}, $d_{\alpha N}(i,i+2)$, and $D_{\alpha N}(i,i+3)$ NOEs (Pelton et al., 1991). $^{13}C\alpha$ signals for the four sequential residues (Val-39–Ala-42) within region HI and the first five residues (Pro-125–Glu-129) within region HIII showed downfield shifts with respect to random coil values characteristic of α-helices or 3_{10} helices (3.0 ppm). However, if the shifts are averaged over the length of each region, the downfield deviations for HI (1.4 ppm), HII (1.0 ppm), HIII (1.6 ppm), and HIV (0.2 ppm) are much lower. It is also interesting to note that the amide proton exchange rates for Leu-126 and Leu-127 are significantly slower than for the other residues in the four helix-containing regions. These observations suggest that, with the exception of segments (Val-39–Ala-42) and (Pro-125–Glu-129), regions HI–HIV contain distorted helices or loops. This must be particularly true of region HIV, which showed a very small average deviation. In addition, we believe the helical regions of III^{Glc} do not contain undistorted α-helices because virtually no $d_{\alpha\beta}(i,i+3)$ NOEs are observed in ^{13}C NOESY-HMQC spectra of the protein (Pelton et al., 1991). A more precise characterization of the helix-containing regions, particularly the distinction between short helices and turns or loops must await determination of the 3D structure. Finally, we note that the deviations of $^{13}C\alpha$ and $^{13}C\beta$ signals with respect to random coil chemical shifts for residues in the 11 strands of antiparallel β-sheet (Pelton et al., 1991) are in agreement with the predicted trends (Spera & Bax, 1991).

The ^1H, ^{15}N, and ^{13}C assignments reported in Table I provide a starting point for NMR studies of the structure and function of III^{Glc}. For a protein of this size, the ^{15}N and ^{13}C assignments are particularly useful since they can be used to distinguish overlapping ^1H resonances through application of multidimensional NMR experiments. The heteronuclear assignments were already of value in determination of the secondary structure of III^{Glc} (Pelton et al., 1991) and open the way to further structural analysis through application of both 3D ^{15}N and ^{13}C NOESY-HMQC spectra and 4D NOESY-HMQC spectra (Kay et al., 1990c; Clore et al., 1991). The heteronuclear assignments also make possible the study of internal protein dynamics by means of relaxation and hydrogen-exchange measurements and the effects of modifications and mutations of III^{Glc} that directly relate to its function (Presper et al., 1989). Finally, the particular strategy for protein assignment used here as well as that of Ikura et al. (1990c, 1991) should promote efforts toward automation of protein assignments and lay the ground work for analyzing still larger systems by NMR spectroscopy.

After the original manuscript was submitted, we received a model for the structure of III^{Glc} based on X-ray crystallographic data (Worthylake et al., 1991). The NMR data presented herein are consistent with those results.

Added in Proof

^{15}N and ^1H NMR signal assignments and secondary structure were recently reported for the C-terminal domain of the *B. subtilis* glucose permease (IIa) which has 42% sequence identity with *E. coli* III^{Glc} and functions in a similar manner (Fairbrother et al., 1991).

Acknowledgments

We acknowledge Drs. A. Bax, D. Garrett, M. Ikura, L. Kay, and D. Marion for providing pulse sequences and computer software needed to process the 3D data sets. We thank R. Tschudin and R. Rendle for expert technical support.

Supplementary Material Available

Five figures containing ^{15}N–^1H HSQC spectra of $III^{Glc}N$ and $III^{Glc}SL$, ^{13}C HMQC spectra of $III^{Glc}SL$ showing Gly, Phe, Pro, and Ser ^{13}C–^1H signals, ^{13}C HMQC-NOESY spectrum of $III^{Glc}SL$ showing $^{13}C\beta$–$H\beta$ to 2,6H NOEs, and the downfield region of a homonuclear TOCSY spectrum of $III^{Glc}SL$ (5 pages). Ordering information is given on any current masthead page.

References

Arrowsmith, C. H., Pachter, R., Altman, R. B., Iyer, S. B., & Jardetzky, O. (1990) *Biochemistry 29*, 6332–6341.

Bax, A. (1989) *Annu. Rev. Biochem. 58*, 223–256.

Bax, A., & Davis, G. (1985) *J. Magn. Reson. 65*, 355–360.

Bax, A., & Ikura, M. (1991) *J. Biol. Nucl. Magn. Reson. 1*, 99–104.

Bax, A., Clore, G. M., Driscoll, P. C., Gronenborn, A. M., Ikura, M., & Kay, L. E. (1990a) *J. Magn. Reson. 87*, 620–627.

Bax, A., Clore, G. M., & Gronenborn, A. M. (1990b) *J. Magn. Reson. 88*, 425–431.

Bax, A., Ikura, M., Kay, L. E., Torchia, D. A., & Tschudin, R. (1990c) *J. Magn. Reson. 86*, 304–318.

Braunschweiler, L., & Ernst, R. R. (1983) *J. Magn. Reson. 53*, 521–528.

Clore, G. M., & Gronenborn, A. M. (1989) *CRC Crit. Rev. Biochem. Biol. 24*, 479–564.

Clore, G. M., & Gronenborn, A. M. (1991) *Science 252*, 1390–1399.

Clore, M. G., Bax, A., Driscoll, P. C., Wingfield, P. T., & Gronenborn, A. M. (1990) *Biochemistry 29*, 8172–8184.

Clore, G. M., Kay, L. E., Bax, A., & Gronenborn, A. M. (1991) *Biochemistry 30*, 12–18.

Cross, T. A., & Opella, S. J. (1985) *J. Mol. Biol. 182*, 367–381.

Dörschug, M., Frank, R., Kalbitzer, H. R., Hengstenberg, W., & Deutscher, J. (1984) *Eur. J. Biochem. 144*, 113–119.

Fairbrother, W. J., Cavanagh, J., Dyson, H. J., Palmer, A. G., Sutrina, S. L., Reizer, J., Saier, M. H., & Wright, P. E. (1991) *Biochemistry 30*, 6896–6907.

Fesik, S. W., & Zuiderweg, E. R. P. (1988) *J. Magn. Reson. 78*, 588–593.

Griffey, R. H., & Redfield, A. G. (1987) *Q. Rev. Biophys. 19*, 51–82.

Gronenborn, A. M., Bax, A., Wingfield, P. T., & Clore, G. M. (1989) *FEBS Lett. 243*, 93–98.

Howarth, O. W., & Lilley, D. M. (1978) *Progress in NMR Spectroscopy* (Emsley, J. W., Feeney, J., & Sutcliff, L. H., Eds.) Vol 12, pp 1–40, Pergamon Press, New York.

Ikura, M., Kay, L. E., Tschudin, R., & Bax, A. (1990a) *J. Magn. Reson. 86*, 204–209.

Ikura, M., Krinks, M., Torchia, D. A., & Bax, A. (1990b) *FEBS Lett. 266*, 155–158.

Ikura, M., Kay, L. E., & Bax, A. (1990c) *Biochemistry 29*, 4659–4667.

Ikura, M., Kay, L. E., Krinks, M., & Bax, A. (1991) *Biochemistry 30*, 5498–5504.

Kainosho, M., & Tsuji, T. (1982) *Biochemistry 21*, 6273–6279.
Kalbitzer, H. R., Deutscher, J., Hengstenberg, W., & Rösch, P. (1981) *Biochemistry 20*, 6178–6185.
Kalbitzer, H. R., Hengstenberg, W., Rösch, P., Muss, H. P., Bernsmann, R., & Dörschug, M. (1982) *Biochemistry 21*, 2879–2885.
Kalbitzer, H. R., Muss, H. P., Engelmann, R., Kiltz, H. H., Stuber, K., & Hengstenberg, W. (1985) *Biochemistry 24*, 4562–4589.
Kaptein, R., Boelens, R., Scheek, R. M., & van Gunsteren, W. F. (1988) *Biochemistry 27*, 5389–5395.
Kay, L. E., Marion, D., & Bax, A. (1989) *J. Magn. Reson. 84*, 72–84.
Kay, L. E., Ikura, M., Tschudin, R., & Bax, A. (1990a) *J. Magn. Reson. 89*, 496–514.
Kay, L. E., Ikura, M., & Bax, A. (1990b) *J. Am. Chem. Soc. 112*, 888–889.
Kay, L. E., Clore, M. G., Bax, A., & Gronenborn, A. M. (1990c) *Science 249*, 411–414.
Klevit, R. E., & Drobny, G. (1986) *Biochemistry 25*, 7769–7773.
Klevit, R. E., & Waygood, E. B. (1986) *Biochemistry 25*, 7774–7781.
Klevit, R. E., Drobny, G., & Waygood, E. B. (1986) *Biochemistry 25*, 7760–7769.
LeMaster, D. M. (1987) *FEBS Lett. 223*, 191–196.
LeMaster, D. M., & Richards, F. M. (1988) *Biochemistry 27*, 142–150.
Levy, G. C., & Nelson, G. L. (1972) *^{13}C NMR for Organic Chemists*, Wiley-Interscience, New York.
Live, D. H., Davis, D. G., Agosta, W. C., & Cowburn, D. (1984) *J. Am. Chem. Soc. 106*, 1939–1941.
McIntosh, L. P., Wand, A. J., Lowry, D. F., Redfield, A. G., & Dahlquist, F. W. (1990) *Biochemistry 29*, 6341–6362.
Marion, D., Kay, L. E., Sparks, S. W., Torchia, D. A., & Bax, A. (1989a) *J. Am. Chem. Soc. 111*, 1515–1517.
Marion, D., Driscoll, P. C., Kay, L. E., Wingfield, P. T., Bax, A., Gronenborn, A. M., & Clore, G. M. (1989b) *Biochemistry 28*, 6150–6156.
Marion, D., Ikura, M., Tschudin, R., & Bax, A. (1989c) *J. Magn. Reson. 85*, 393–399.
Marion, D., Ikura, M., & Bax, A. (1989b) *J. Magn. Reson. 84*, 425–430.
Meadow, N. D., & Roseman, S. (1982) *J. Biol. Chem. 257*, 14526–14537.
Meadow, N. D., Coyle, P., Komoryia, A., Anfinsen, C. B., & Roseman, S. (1986) *J. Biol. Chem. 261*, 13504–13509.
Meadow, N. D., Fox, D. K., & Roseman, S. (1990) *Annu. Rev. Biochem. 59*, 497–542.
Neidhardt, F. C., Block, P. L., & Smith, D. F. (1974) *J. Bacteriol. 119*, 736–747.
Niemczura, W. P., Helms, G. L., Chesnick, A. S., Moore, R. E., Bornemann, V. (1989) *J. Magn. Reson. 81*, 635–640.
Oh, B. H., Westler, W. M., Derba, P., & Markley, J. L. (1988) *Science 240*, 908–911.
Oppenheimer, N. J., & James, T. L., Eds. (1989) *Methods Enzymol. 176, 177.*
Oschkinat, H., Griesinger, C., Kraulis, P. J., Sorensen, O. W., Ernst, R. R., Gronenborn, A. M., & Clore, G. M. (1988) *Nature (London) 332*, 374–377.
Oschkinat, H., Cieslar, C., Gronenborn, A. M., & Clore, G. M. (1989) *J. Magn. Reson. 81*, 212–216.
Pelton, J. G., Torchia, D. A., Meadow, N. D., Wong, C.-Y., & Roseman, S. (1991) *Proc. Natl. Acad. Sci. U.S.A. 88*, 3479–3483.
Postma, P. W., & Lengeler, J. (1985) *Microbiol. Rev. 49*, 232–269.
Presper, K. A., Wong, C.-Y., Liu, L., Meadow, N. D., & Roseman, S. (1989) *Proc. Natl. Acad. Sci. U.S.A. 86*, 4052–4055.
Rance, M., Sorensen, O. W., Bodenhausen, G., Wagner, G., Ernst, R. R., & Wüthrich K. (1983) *Biochem. Biophys. Res. Commun. 117*, 479–485.
Roseman, S., & Meadow, N. D. (1990) *J. Biol. Chem. 265*, 2993–2996.
Saier, M. H., Jr. (1989) *Microbiol. Rev. 53*, 109–120.
Saitô, H., & Ando, I. (1989) *Annu. Rep. Nucl. Magn. Reson. Spectrosc. 21*, 252–253.
Shaka, A. J., Keeler, J., & Freeman, R. (1983) *J. Magn. Reson. 53*, 313–340.
Shaka, A. J., Barker, P., & Freeman, R. (1985) *J. Magn. Reson. 64*, 547–552.
Shaka, A. J., Lee, C. J., & Pines, A. (1988) *J. Magn. Reson. 77*, 274–293.
Shon, H., & Opella, S. J. (1989) *J. Magn. Reson. 82*, 193–197.
Spera, S., & Bax, A. (1991) *J. Am. Chem. Soc. 113*, 5490–5492.
Stockman, B. J., Westler, W. M., Prashanth, D., & Markley, J. L. (1988) *J. Am. Chem. Soc. 110*, 4095–4096.
Stockman, B. J., Reilly, M. D., Westler, W. M., Ulrich, E. L., & Markley, J. L. (1989) *Biochemistry 28*, 230–236.
Studier, F. W., & Moffatt, B. A. (1986) *J. Mol. Biol. 189*, 113–130.
Torchia, D. A., Lyerla, J. R., & Quattrone, A. J. (1975) *Biochemistry 14*, 887–900.
Torchia, D. A., Sparks, S. W., & Bax, A. (1988) *Biochemistry 27*, 5135–5141.
Torchia, D. A., Sparks, S. W., & Bax, A. (1989a) *J. Am. Chem. Soc. 110*, 2320–2321.
Torchia, D. A., Sparks, S. W., & Bax, A. (1989b) *Biochemistry 28*, 5509–5524.
Vuister, G. W., Boelens, R., & Kaptein, R. (1989) *J. Magn. Reson. 80*, 176–185.
Wagner, A., & Bruehwiler, D. (1986) *Biochemistry 25*, 5839–5843.
Westler, W. M., Kainosho, M., Nagao, H., Tomonaga, N., & Markley, J. L. (1988) *J. Am. Chem. Soc. 110*, 4093–4095.
Worthylake, D., Meadow, N. D., Roseman, S., Liao, D., Hertzberg, O., & Remington, S. J. (1991) *Proc. Natl. Acad. Sci. U.S.A.* (in press).
Wüthrich, K., (1986) *NMR of Proteins and Nucleic Acids*, Wiley, New York.
Zuiderweg, E. R. P., & Fesik, S. W. (1989) *Biochemistry 28*, 2387–2391.